

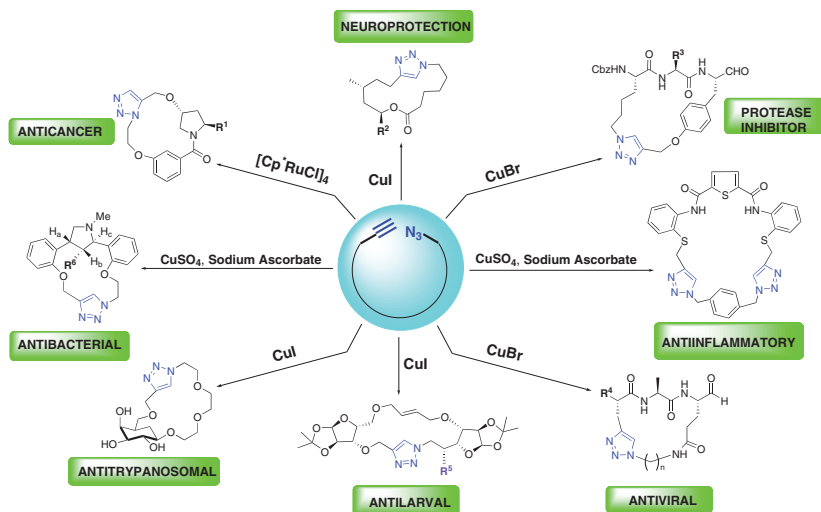
Synthesis of Bioactive 1,2,3-Triazole-Fused Macrocycles via Azide-Alkyne Cycloaddition

Nasrin Jahan

Arkadip Pal

Inul Ansary*

Department of Chemistry, The University of Burdwan,
Burdwan 713104, India
iansary@chem.buruniv.ac.in



Received: 17.10.2023

Accepted after revision: 15.11.2023

Published online: 16.11.2023 (Accepted Manuscript), 04.01.2024 (Version of Record)

DOI: 10.1055/a-2212-0996; Art ID: SO-2023-10-0076-RV

License terms:

© 2024. The Author(s). This is an open access article published by Thieme under the terms of the Creative Commons Attribution License, permitting unrestricted use, distribution and reproduction, so long as the original work is properly cited. (<https://creativecommons.org/licenses/by/4.0/>)

Abstract A systematic highlight of syntheses reported since 2006 of 1,2,3-triazole-fused macrocycles possessing biological activities such as anticancer, antibacterial, antiviral, anti-inflammatory and antilarval action, is presented in this review. The well-renowned Cu-catalyzed azide-alkyne cycloaddition reaction was noted to be highly efficient and is one the most common methods utilized by scientists for the synthesis of 1,4-disubstituted triazole-fused macrocycles, whereas Ru-catalyzed cycloaddition is common for the formation of 1,5-disubstituted bioactive triazoles. This review would thus be extremely beneficial for both synthetic organic and medicinal chemists.

- 1 Introduction
- 2 Anticancer Derivatives
- 3 Antibacterial Derivatives
- 4 Derivatives with Dual Activity
- 5 Antilarval Derivatives
- 6 Anti-inflammatory Derivatives
- 7 Antiviral Derivatives
- 8 Anti-trypanosomal Derivatives
- 9 Derivatives with Miscellaneous Activities
- 10 Conclusion

Key words triazole, macrocycles, anticancer, antibacterial, antiviral, bioactivity

1 Introduction

Over a long period, the evolution of therapeutic compounds required for treatment of a wide range of diseases has revolved around the construction of various natural products as well as their synthetic analogues. Based on their improved physicochemical potential and pharmacokinetics compared with acyclic molecules, macrocycles have provided continuously emerging targets for drug discovery despite their synthetic challenges.^{1,2} Macrocyclic compounds have been reported to display a wide range of bioactivities viz. anticancer, antibacterial, antifungal, immunosuppressant and more, and thus have proven themselves to be extremely effective in the field of medicine.³ In particular, 1,2,3-triazole-fused macrocycles have exhibited promising biological activities such as anticancer,^{4–6} antibacterial,⁷ anti-inflammatory,⁸ antiviral,⁹ and more;^{10–12} hence, the synthesis of triazole-based macrocycles has become a hot topic for researchers. Published reports revealed that significant efforts have been made towards the synthesis of triazole scaffolds involving Ag(I)-, Cu(I)-, and Ru(II)-catalyzed azide-alkyne cycloaddition (AAC) reactions, microwave-assisted reactions, and ultrasound-promoted reactions etc.¹³ The deep impact of the well-renowned Cu(I)-catalyzed azide-alkyne cycloaddition (CuAAC) reaction upon synthetic organic chemistry has persuaded several researchers to utilize this reaction while developing the triazole-based analogues of naturally occurring macrocyclic compounds. Through a literature survey, we realized that no recent re-

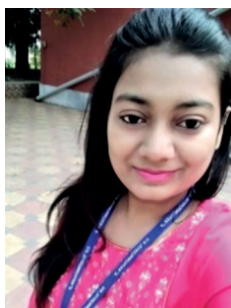
view on the synthesis of bioactive 1,2,3-triazole fused macrocycles was available. Being currently engaged in the synthesis of macrocycles,¹⁴ we herein report a review article summarizing the synthetic protocols undertaken to construct bioactive triazole-fused macrocycles since 2006. Throughout the article, we focus on CuAAC and RuAAC reactions that have been utilized for the preparation of 1,2,3-triazoles. We are optimistic that this review will be extremely beneficial for synthetic organic and medicinal chemistry researchers and will provide guidance on the development of novel macrocycles that are essential for drug discovery.

2 Anticancer Derivatives

In order to combat a worldwide health problem – cancer – researchers have paid avid attention towards the two ‘D’s in therapeutic development: Detection and Diagnosis. Early detection of this fatal disease is essential for appropriate diagnosis and the needs of the affected people could only be met through proper treatment *via* medicinal resources. Scientists have devoted countless numbers of years in cancer therapy to not just curing patients but also to improving their quality of life post-treatment.

Continuous activation of signal transducers and activators of transcription 3 (STAT3) has been directly linked to

Biographical Sketches



Nasrin Jahan was born in 1993 in Durgapur, West Bengal, India. She graduated in Chemistry (2015) from the University of Burdwan, West Bengal, India

and obtained her M.Sc. degree (2017) from Kazi Nazrul University, West Bengal, India. Currently, she is pursuing her Ph.D. degree in synthetic organic

chemistry at the University of Burdwan under the supervision of Dr. Inul Ansary.



Arkadip Pal was born in Malda, West Bengal, India, in 1999. He is an INSPIRE Scholar under DST and obtained his B.Sc. (Hons.) degree in 2021 from

Bankura University, West Bengal, India. Subsequently, he obtained his M.Sc. degree in Chemistry in 2023 from The University of Burdwan, West

Bengal, India, and completed his project-based term paper under the supervision of Dr. Inul Ansary for the fulfilment of his final semester examination.



Dr. I. Ansary was born in 1983 in Raghunathpur, Purulia, West Bengal, India. He obtained his B.Sc. in Chemistry (2004) from The University of Burdwan, Burdwan, India and his M.Sc. degree (2006) from the University of Calcutta, Kolkata, India. He received his Ph.D. in Chemistry (July, 2013) under the supervision of Dr. B. Roy from the University of Kalyani. He joined as an Assistant Professor in Chemistry in November 2012 at The

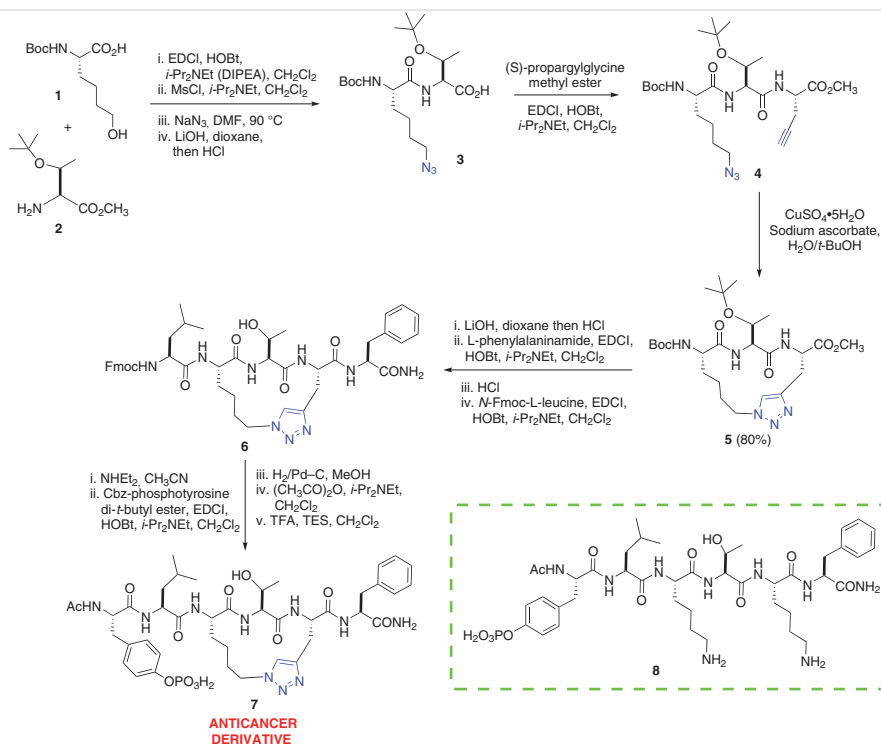
University of Burdwan, West Bengal and teaches Organic Chemistry in the postgraduate level. His research interests are in the areas of development of new synthetic routes and methodologies to construct nitrogen and oxygen heterocycles of different ring sizes and their application on the basis of molecular modeling and docking studies. Recently, he has been working in the field of pesticide residue analysis. He has published 30

research articles, 1 review and 2 book chapters. He also reviewed several research articles in internationally reputed journals. Under his supervision two students have been awarded Ph.D. degree and currently three students are still working in his group. He also supervised more than 50 M.Sc. students who successfully submitted their project-based term papers.

oncogenesis and the process serves as a target for molecular drug design. In 2007, Chen *et al.* designed a conformationally constrained macrocycle **7** by following the 'click-chemistry' methodology as a crucial step (Scheme 1).¹⁵ The synthetic procedure advanced with the condensation between Boc-L-6-hydroxynorleucine **1** and *O*-*t*-butyl-L-threonine methyl ester **2**, in the presence of 1-ethyl-3-(3-dimethylaminopropyl)carbodiimide (EDCI), hydroxybenzotriazole (HOBt) and *N,N*-diisopropylethylamine (DIPEA) in dichloromethane. Three consecutive steps provided the azide moiety **3**, which was further converted into the macrocyclic precursor **4** via condensation with (*S*)-propargylglycine methyl ester. On constituting both the azide-alkyne groups within itself, **4** was subjected to an intramolecular copper(I)-catalyzed azide-alkyne cycloaddition (CuAAC) reaction in the presence of copper sulfate and sodium ascorbate in a *t*-BuOH/*H*₂O solvent system to furnish the 1,4-disubstituted triazole-fused macrocycle **5** in 80% yield. This key intermediate was further exposed to nine more sequential reactions to afford the target macromolecule **7**. A fluorescence-polarization-based binding assay was conducted next to confirm that **7** expressed an effective binding affinity with STAT3 and was found to be more potent when compared with the peptide **8**. The target drug **7** was thus established to be an anticancer agent with a strong inhibition of STAT3.

Histone deacetylases (HDACs) are enzymes that play an important part in the regulation of gene transcription and,

over the years, inhibition of HDACs have resulted in the evolution of anticancer chemotherapy. Apicidin, a naturally occurring cyclic tetrapeptide, was found to exhibit cytotoxic activity by inhibiting the action of HDACs. In 2009, Horne *et al.* developed few triazole-modified apicidin analogues **16a**, **b**, **17**, **25a–c** and carried out the HDAC inhibition assay (Scheme 2 and Scheme 3).⁴ The synthetic procedure commenced with the preparation of the two key fragments, **11** and **14**, from the starting materials bromoketal **9** and the Boc-protected lactone **12**, respectively. Compound **9** was initially converted into the Grignard derivative and then reacted with the lactone **10** to produce the amino acid derivative **11**. The synthesis of the alkyne moiety **14** proceeded with the conversion of the Boc-protected lactone **12** into the acid **13**, which was further subjected to a three-step reaction. The two synthons **11** and **14** were exposed to solution-phase peptide synthesis *via* six sequential reactions to prepare the azide-alkyne cycloaddition precursors **15a** and **15b**, which finally underwent intramolecular cycloaddition using catalytic CuI, 2,6-lutidine, tris(benzyltriazolylmethyl)amine (TBTA) and DIPEA in acetonitrile for 48 h to afford the desired 1,4-disubstituted triazole fused macrocycles **16a** and **16b**, respectively. The macrocyclic precursor **15a** was alternatively exposed to microwave conditions in DMF at 220 °C, which led to the production of a mixture of 1,5-disubstituted triazole fused macrocycle **17** (8%) and macrocycle **16a** in a 2:1 ratio (Scheme 2). Next, multiple conformations of **17** were investigated by replacing the β -substi-



Scheme 1 Synthesis of STAT3 inhibitor **7**

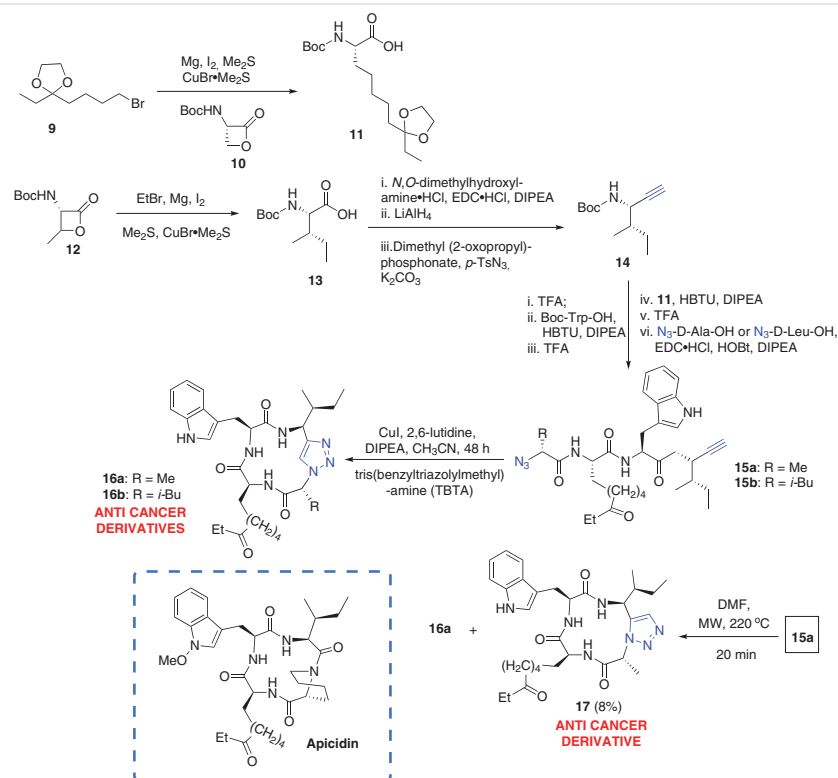
tuted amino acid Ile with a Leu residue. The Fmoc-protected 2-amino 8-oxodecanoic acid (Aoda) on resin **18** was treated with piperidine to remove the protection and subsequently the de-protected **19** was coupled with the N_3 -Ala-OH (D/L) **20** to afford the amide **21**. To ensure the intermolecular cycloaddition reaction, the azido-amide **21** and Fmoc-Leu-CCH (D/L) **22** were treated with a Ru-based catalyst $[Cp^*Ru(cod)Cl]$ in toluene at 45 °C for 16 h and the triazole-moiety **23** was afforded. Four subsequent steps led to the formation of the linear pseudotetrapeptides **24a–c**, which finally underwent macrolactamization through HATU peptide coupling to afford the desired macrocycles **25a–c**, differing at the Ala and Leu positions, in yields greater than 95% (Scheme 3). The bioactivities of all the apicidin analogues were assessed in nuclear extracts of HeLa cells and they were found to exhibit HDAC inhibitor activity.

In 2010, the McAlpine group synthesized a set of macrocyclic triazole derivatives **33** and assessed their HDAC inhibitory activity (Scheme 4).¹⁶ The synthetic procedure commenced with the conversion of aldehyde **26** into alkyne **27** with Bestmann–Ohira reagent. Four sequential reactions involving condensation of **27** with the Boc-protected amino acids **28** and **29** resulted in the development of the residue **30**, which was, in turn, HATU/TBTU coupled with azide **31** to afford the linear precursor **32**. Finally, the crucial macrocyclization step was undertaken via CuAAC reaction using

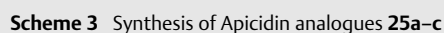
copper sulfate and sodium ascorbate in a methanol/water solvent system to afford the desired macrocycles **33** in 3–9% yield. The biological evaluation of these compounds revealed inhibition of deacetylase activity against HeLa cell lysates. Compounds **33a** and **33b** were found to be the most potent.

The Sewald group, in 2010, developed a bioactive triazole analogue **44** of the antitumor agent ‘Cryptophycin-52’ using the Cu-mediated cycloaddition reaction as one of the crucial steps (Scheme 5 and Scheme 6).¹⁷ The synthesis advanced with the creation of alkyne **35** in two steps from the starting material **34**. The other building block **38** was afforded through condensation of acid **36** and alcohol **37** and was subsequently exposed to CuAAC reaction using CuI and DIPEA in DMF for 14 h at ambient temperature for the construction of the triazole **39** (Scheme 5).

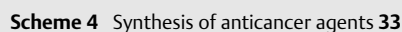
Hydrogenolytic deprotection of the Bn group in **39** with subsequent esterification with the alcohol moiety **40** resulted in the formation of the macrocyclic precursor **41**. Final cleavage of the protecting groups with macrocyclization under pseudo-high-dilution conditions furnished the key intermediate **42** in 74% yield. An alternative procedure to synthesize **42** was also developed from the Boc-deprotected moiety **45** (Scheme 6). Thus, the acid **43** was coupled with the alkyne-amine moiety **45** using EDC/HOBt in order to achieve the amide **46**, which was further subjected to con-

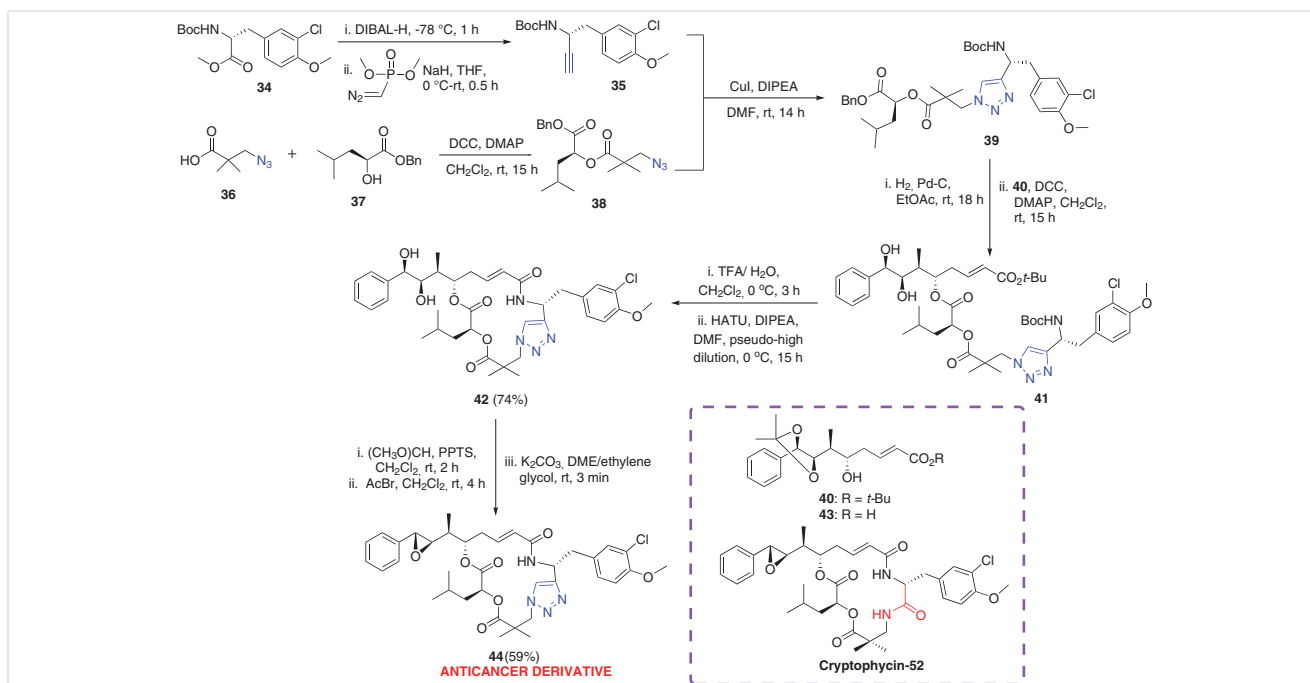


Scheme 2 Synthesis of apicidin analogues **16a,b** and **17**



Pirali *et al.*, in 2010, synthesized certain macrocyclic peptide mimetics **56a,b** and **61a,b** through intramolecular [3+2] cycloaddition and biologically evaluated them as HDAC inhibitors (Scheme 7 and Scheme 8).¹⁸ Initially, the synthetic procedure for the first set of macrocycles commenced with the preparation of the aldehydes **53a,b** from their corresponding alcohols using Dess–Martin reagent through oxidation. With the other fragments α -isocyanoacetamide **51** and the amine **52** in hand, a three-component reaction was conducted using NH_4Cl as a catalyst to afford the 5-aminooxazole **54a,b**. Subsequently, the crucial mac-

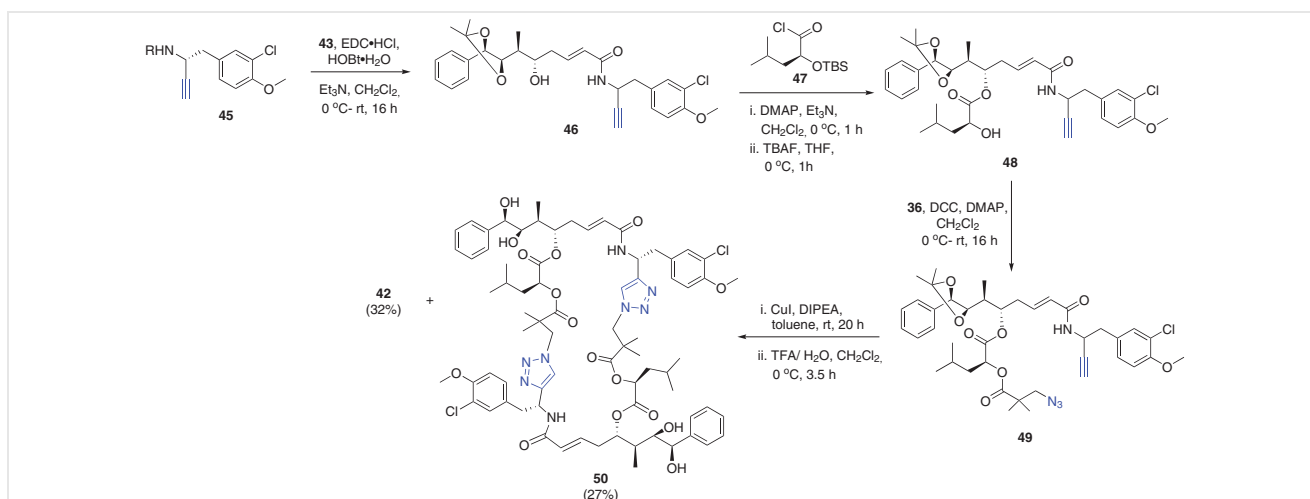


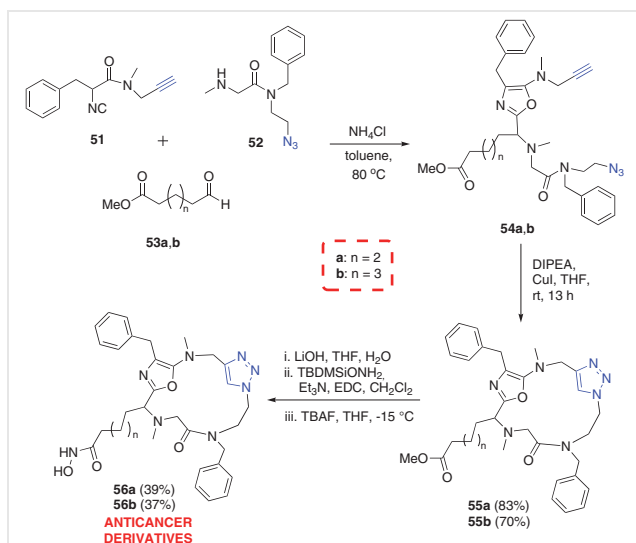
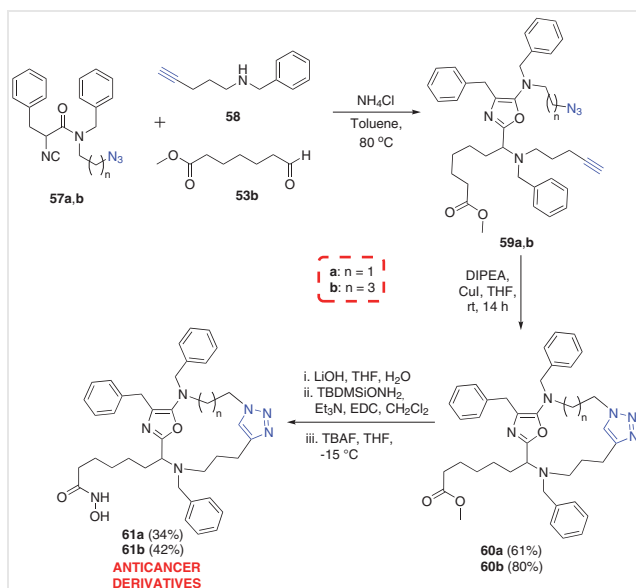


rocyclization step was carried out *via* CuAAC reaction with catalytic CuI and DIPEA in THF at room temperature for 13 h in order to furnish the macrocycles **55a** and **55b** in 83% and 70% yields, respectively (Scheme 7).

Three subsequent reactions upon **55a,b** afforded the targeted hydroxamic macrocycles **56a,b** in 39% and 37% yield, respectively. To generate the second set of macrocycles, a similar ammonium chloride catalyzed methodology was followed using the aldehyde **53b**, the alkyne **58**, and the azides **57a,b** as starting materials for the development

of the macrocyclic precursors **59a,b** (Scheme 8). A CuI supported cycloaddition following the aforementioned method took place next to graft the macrocycles **60a** and **60b** in 61% and 80% yields, respectively. Finally, the desired hydroxamic compounds **61a,b** were synthesized in 34% and 42% yields in three subsequent steps. Biological evaluation of **56a,b** and **61a,b** through MTT assay determined their inhibitory activity in SHSY-5Y cells. It was further predicted through molecular docking that **55b** and **61b** would display inhibition of histone deacetylases.



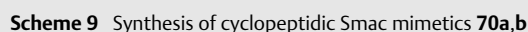
Scheme 7 Synthesis of macrocyclic peptide mimetics **56a,b**Scheme 8 Synthesis of macrocyclic peptide mimetics **61a,b**

In the same year, Sun *et al.* synthesized the cyclopeptidic Smac mimetics **70a,b** utilizing the CuAAC reaction as the macrocyclization pathway and evaluated their anticancer activities (Scheme 9).¹⁹ The process was initiated with the condensation of L-proline benzyl ester hydrochloride **62** and N-Boc-L-6-hydroxynorleucine to achieve the amide **63**. Mesylation of **63**, followed by treatment with sodium azide, afforded the azido derivative **64**, which was further subjected to azide-alkyne cycloaddition with **65a/65b** to graft the key intermediates **66a,b**, respectively. Four subsequent reaction steps resulted in the development of the macrocyclic precursors **67a,b**, which underwent the crucial Cu-cata-

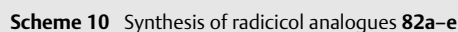
lyzed AAC reaction with copper sulfate and sodium ascorbate in *t*-BuOH/H₂O medium to synthesize the macrocycles **68a** (38%) and **68b** (35%), respectively. After removing the protecting groups, condensation was carried out between **69a,b** and N-methyl-N-Boc-L-alanine to construct the amides. Ultimate Boc deprotection afforded the desired compounds **70a** (79%) and **70b** (72%), which were further biologically evaluated. Through an FP-based binding assay, it was found that the binding affinity of **70a** was more than that of **70b** towards binding to XIAP, cIAP-1 and cIAP-2 proteins. When the inhibition activity of the target macrocycles was evaluated against growth of MDA-MB-231 breast cancer and SK-OV-3 ovarian cancer cell lines, compound **70a** was reported to be more potent than parent compound **71**, whereas **70b** was noted to be weaker than **71**.

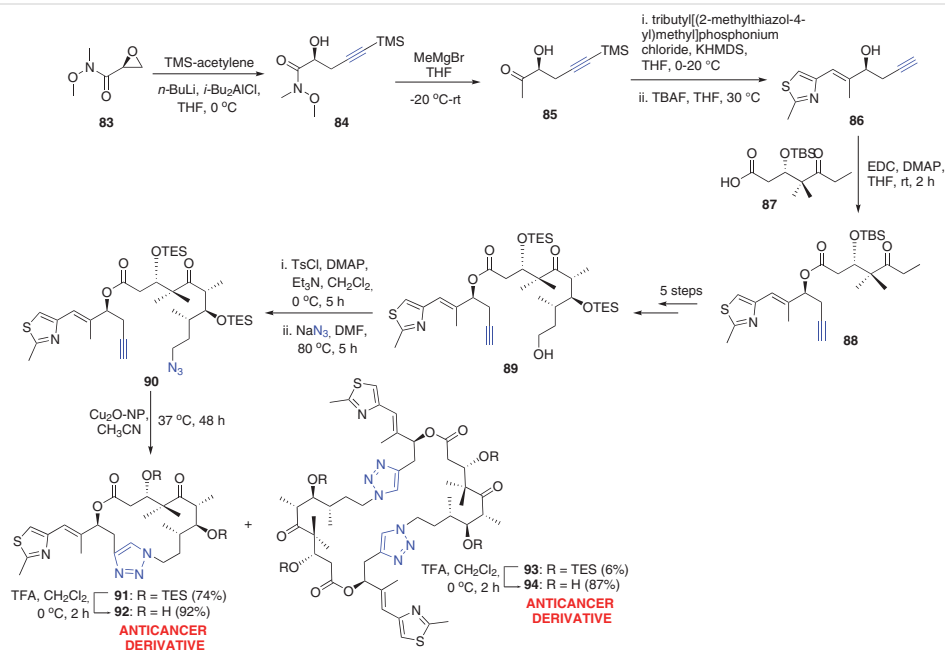
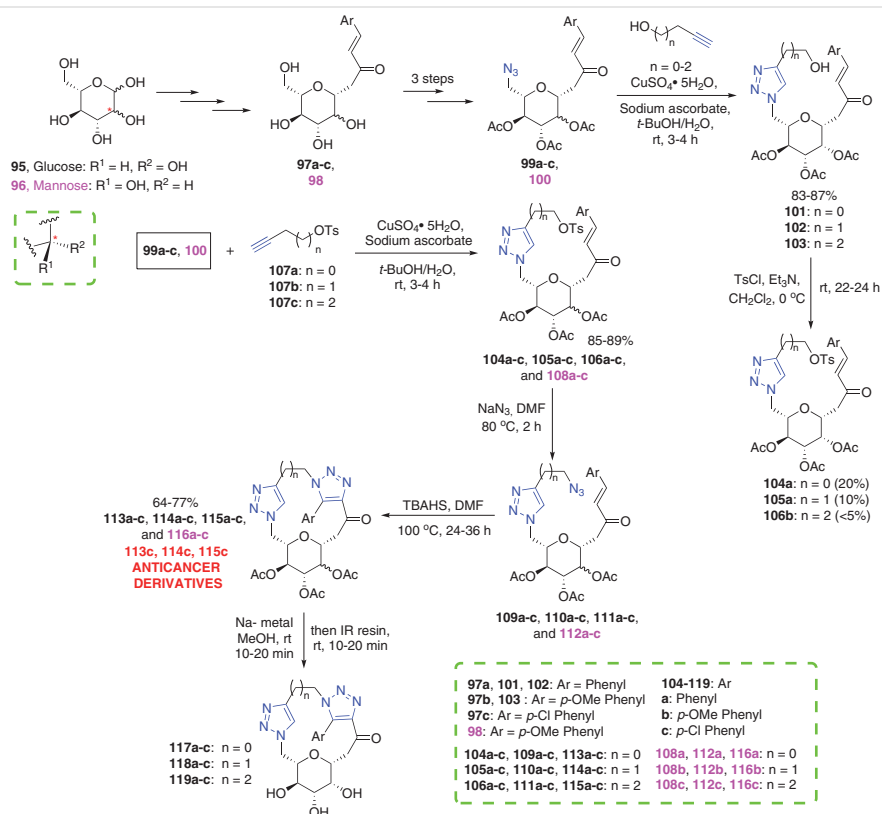
Heat shock protein 90 (Hsp90) is a captivating target for medicinal chemists with respect to cancer therapy. Day *et al.*, in 2010, synthesized a series of macrocyclic analogues (**82a–e**) of the naturally occurring Hsp90 inhibitor 'radicol' (Scheme 10).⁵ The synthetic route advanced with the conversion of 4-chlororesorcinol **72** into the homophthalate ester **73** in two steps, which further underwent six reactions to afford the intermediate **74**. The substituted diethyl malonates **75a–d** were next transformed into their corresponding acid chlorides **76a–d** by treatment with thionyl chloride. Subsequently, the chlorides **76a–d** were coupled with the anhydride **74**, using tetramethylguanidine (TMG), to produce **77a–d**, which were eventually transformed into the isocoumarins **78a–d**. Treatment of **78b–d** with excess lithium hydroxide resulted in their ring-opening to give the alkyne moieties **79a–e**, which were subsequently treated with either 2-azidoethanol or 3-azidopropanol under Mitsunobu conditions to achieve the macrocyclic precursors **80a–e**. The crucial macrocyclization took place using copper sulfate and sodium ascorbate in *t*-BuOH/H₂O medium to afford the macrocyclic triazoles **81a–e** in 8–33% yields. Final deprotection of the MOM groups was conducted with TFA in dichloromethane to furnish the desired compounds **82a–e** in 21–84% yields. Biological evaluation of **82a–e** for Hsp90 inhibition showed reduced binding activity with loss of potency when compared with radicol and analogue NP261.

In 2012, Duan *et al.* synthesized a triazole-fused analogue of epothilone **92** and reported its computational docking studies (Scheme 11).⁶ Initially, the Weinreb amide **83** was used to prepare fragment **84**, which was later made to react with a Grignard reagent to afford the keto-alcohol **85**. Compound **85** underwent subsequent Horner–Wadsworth–Emmons reaction and desilylation to afford alcohol **86**, which was successively coupled with **87** to form alkyne **88**. Five sequential reactions upon **88** furnished intermediate **89** and further treatment with *p*-toluenesulfonyl chloride and sodium azide helped to generate the macrocyclic precursor **90**. The ring-closure was conducted using Cu₂O-nanoparticles in acetonitrile medium at 37 °C to afford the triazole-fused macrocycles **91** (monomer) and **93** (dimer)



ral epothilones. The target molecule **92** was reported to exhibit lower bioactivity against MCF-7 cell lines than epothilone. Interestingly, dimer **94** also showed bioactivity against the same cell lines even though it was about 200 times less potent than the parent compound Epothilone D.

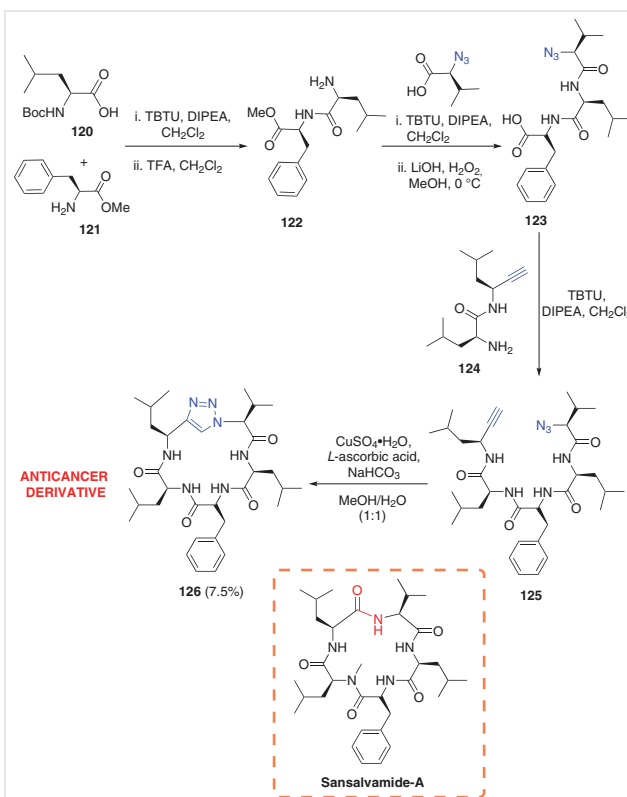


Scheme 11 Synthesis of epothilone analogue **92** and its dimer **94**Scheme 12 Synthesis of macrocyclic glycoconjugates **113c**, **114c** and **115c**

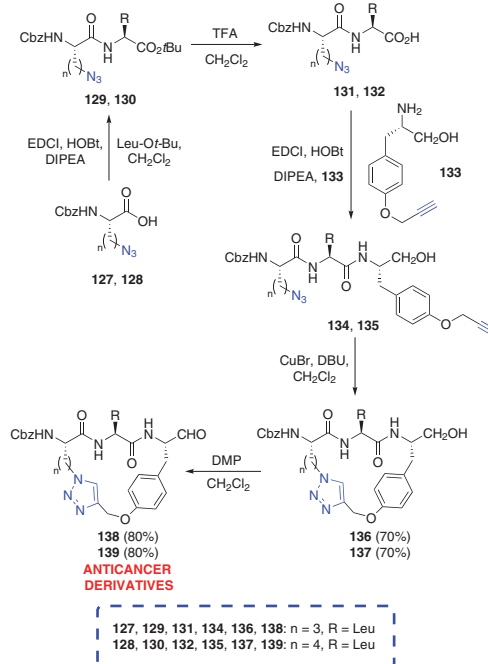
Ajay *et al.*, in 2012, reported the synthesis of some triazole-fused macrocyclic glycoconjugates and also tested their biological activities (Scheme 12).²⁰ The process advanced with the preparation of glycopyranosyl butenones (**97a–c**, **98**) from D-glucose and D-mannose. In three subsequent steps, the azido-glycopyranosyl derivatives (**99a–c**, **100**) were prepared and then subjected to CuAAC reaction with the alkynol moieties in the presence of copper sulfate and sodium ascorbate in *t*-BuOH/H₂O medium at room temperature for 3–4 h, which afforded the triazole derivatives **101–103** in excellent yields (83–87%). Action of tosyl chloride in dichloromethane with triethylamine resulted in the formation of tosylated products **104a**, **105a** and **106b** in poor yields; hence, an alternate pathway for the synthesis of the desired macrocycles was considered. The previously used alkynols were tosylated to create **107a–c** and then made to undergo the CuAAC reaction with **99a–c**, **100** under the previously described reaction conditions to furnish the tosyloxy triazoles **104a–c**, **105a–c**, **106a–c** and **108a–c** in excellent yields (85–89%). Further exposure to sodium azide in DMF at 80 °C formed the macrocyclic precursors **109a–c**, **110a–c**, **111a–c** and **112a–c**, which underwent subsequent macrocyclization using tetrabutylammonium hydrogen sulfate (TBAHS) in DMF at 100 °C for 24–36 h to afford the di-triazole-fused macrocyclic compounds **113a–c**, **114a–c**, **115a–c** and **116a–c** in 64–76% yields. The glucose derived compounds were further deacetylated to afford **117a–c**, **118a–c**, and **119a–c**. On conducting the biological assessment of macrocycles **113a–c**, **114a–c**, **115a–c** and **117a** against breast cancer MCF-7 cell line, compounds **113c**, **114c**, and **115c** were noted to exhibit good to moderate activity.

In 2012, Davis *et al.* developed a peptidomimetic macrocycle **126** through CuAAC methodology, and investigated its bioactivity (Scheme 13).²¹ The synthesis was initiated through the amide coupling of acid **120** and amine **121** in the presence of TBTU and DIPEA. Subsequent acidic deprotection with TFA afforded the key intermediate **122**, which was further subjected with two consecutive reactions to produce the azide **123**. Next, the previously prepared alkyne fragment **124** was further coupled with **123** in the presence of TBTU/DIPEA to achieve the macrocyclic precursor **125**. The key macrocyclization step was finally conducted using L-ascorbic acid, NaHCO₃ and copper sulfate in MeOH/H₂O medium to graft the desired macrocycle **126** (7.5%). The synthesized macrocycle **126** was evaluated in HeLa cervical cancer cell lines and was noted to inhibit the growth. Its level of cytotoxicity was found to be on par with its parent compound Sansalvamide A.

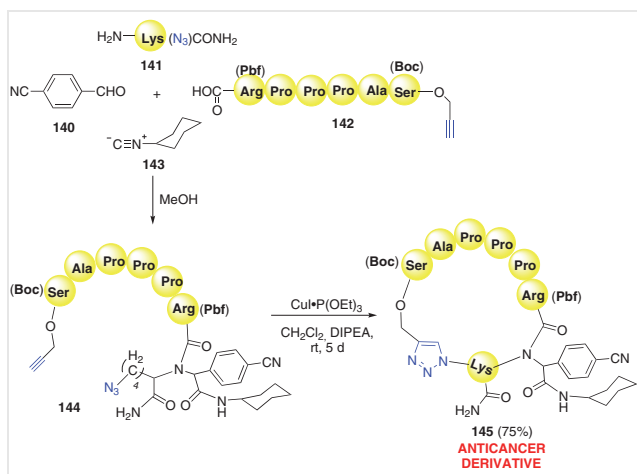
In 2013, Neilsen *et al.* developed two triazole-fused macrocyclic inhibitors (**138**, **139**) of CT-L protease using the Cu-mediated click-methodology in the crucial macrocyclization step (Scheme 14).²² The synthetic procedure advanced with the development of the key azide fragments



Scheme 13 Synthesis of sansalvamide-A analogue **126**



Scheme 14 Synthesis of macrocyclic inhibitors of CT-L protease **138**, **139**

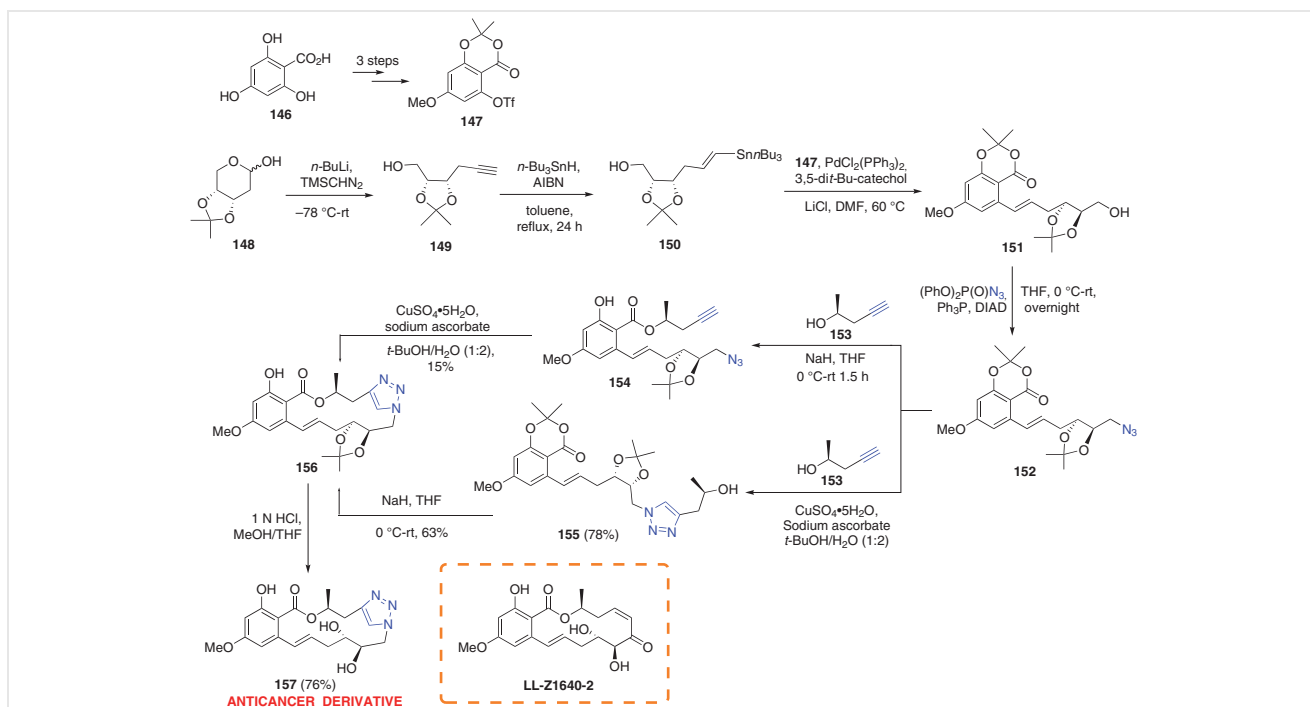
Scheme 15 Synthesis of macrocyclic heptapeptide **145**

129 and **130**, from the starting materials **127**, **128**, under standard amide forming conditions with Leu-*Ot*-Bu using EDCI. Subsequent acidic deprotection led to the formation of **131** and **132**, which were individually coupled with the amino-alkyne moiety **133** under similar EDCI conditions to afford the azide-alkyne containing macrocyclic precursors **134** and **135**. Next, the key macrocyclization step was undertaken in the presence of CuBr and DBU in dichloromethane, which grafted the triazole fused macrocycles **136** and **137** in 70% yields each. Further exposure of these com-

pounds to oxidation with Dess–Martin periodinane (DMP) afforded the aldehyde-based macrocycles **138** and **139** in 80% yields, respectively. Biological evaluation against the protease CT-L showed **138** and **139** both possessed activity as potential inhibitors. The compounds also exhibited potency when tested against a panel of four sarcoma cancer cell lines WE-68, VH-64, STA-ET-1 and TC-252.

Tahoori *et al.*, in 2014, designed a macrocyclic heptapeptide **145** by following Ugi-4CR and Huisgen cycloaddition reactions, and reported its anticancer activity (Scheme 15).²³ To initiate the synthetic process, the 4-cyanobenzaldehyde **140**, azide fragment **141**, the carboxylic acid with a propargyl group **142** and cyclohexyl isocyanide **143** reacted in methanol as a four-component Ugi reaction to afford the macrocyclic precursor **144**. For the click-reaction, CuI·P(OEt)₃ was used as a catalyst with DIPEA in dichloromethane at room temperature for 5 days to obtain the heptapeptidic triazole fused macrocycle **145** in 75% yield. Upon testing its biological properties, macrocycle **145** was seen to exhibit promising anticancer activity against A549 human lung cancer cell line.

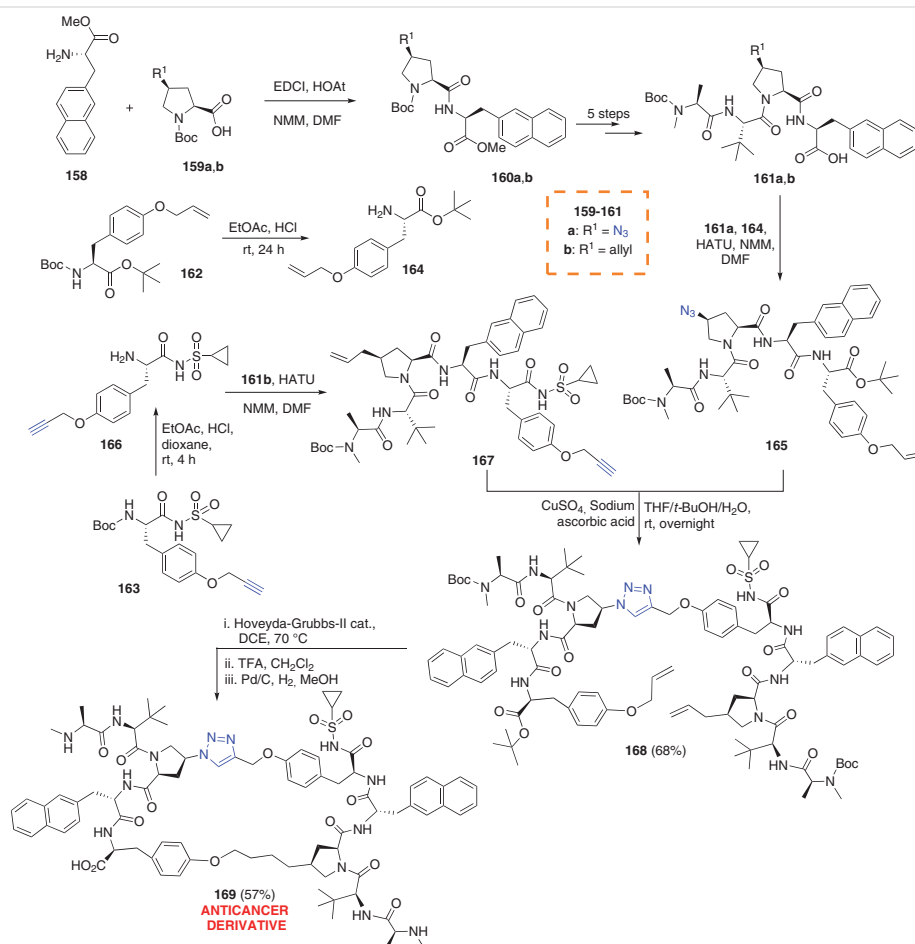
In the same year, Goh *et al.* reported the synthesis of a triazole analogue **157** of natural product LL-Z1640-2 and evaluated its biological activity (Scheme 16).²⁴ Initially, the commercially available 2,4,6-trihydroxybenzoic acid **146** was converted into the triflate **147** in three steps. The reaction progressed as the acetone **148** underwent Colvin rearrangement in the presence of TMS diazomethane and *n*-BuLi to produce the alkyne **149** and further hydrostannyla-

Scheme 16 Synthesis of triazole analogue **157** of natural product LL-Z1640-2

tion produced the *trans*-vinyl stannane **150**. Subsequently, triflate **147** and stannane **150** were subjected to Stille coupling with $\text{PdCl}_2(\text{PPh}_3)_2$ to afford alcohol **151**, which, upon further treatment with diphenylphosphoryl azide, constructed the key azide fragment **152**. Next, the latter was reacted with (*S*)-pent-4-yn-ol **153** in two different pathways; the first reaction was conducted in the presence of NaH to produce the macrocyclization precursor **154**, whereas the second pathway followed standard CuAAC conditions with copper sulfate and sodium ascorbate in *t*-BuOH/ H_2O medium to furnish the triazole **155** in 78% yield. Intramolecular click-reaction of **154** under similar CuAAC conditions established the macrocycle **156** in very poor yield (15%), whereas the intramolecular transesterification of **155** with NaH afforded the desired compound **156** in 63% yield. Final deprotection of **156** by acidification grafted the target triazole analogue **157** in 76% yield. Biological assessment of **157** with several kinases showed its ability to act as a potent inhibitor with an inhibition higher than or comparable to its parent LL-Z1640-2. Besides exhibiting good ac-

tivity against MNK2 kinase, the targeted analogue **157** was also active against AXL and MET and thus, served as a good target for anticancer therapy.

Zhang *et al.*, in 2015, synthesized a dimeric macrocycle **169**, which served as an inhibitor of apoptosis proteins (Scheme 17).²⁵ To initiate the synthetic procedure, commercially available 2-naphthyl alanine **158** was coupled with the prolines **159a,b** using EDCI and HOAt to achieve the compounds **160a,b**, which were further subjected to five successive steps to develop the key fragments **161a,b**. The starting materials **162** and **163** gave rise to the tyrosine derivatives **164** and **166**, which were, in turn, HATU coupled with **161a,b** to afford the pentapeptides **165** and **167**, respectively. The crucial macrocyclization took place between the azide-alkyne fragments **165** and **167** by employing the renowned CuAAC-RCM methodologies. The cycloaddition was conducted overnight at room temperature in the presence of CuSO_4 and sodium ascorbic acid in THF/*t*-BuOH/ H_2O medium to form the triazole linked moiety **168** in 68% yield. Subsequent RCM reaction with Hoveyda-Grubbs-II catalyst, TFA mediated deprotection, and Pd-catalyzed hy-



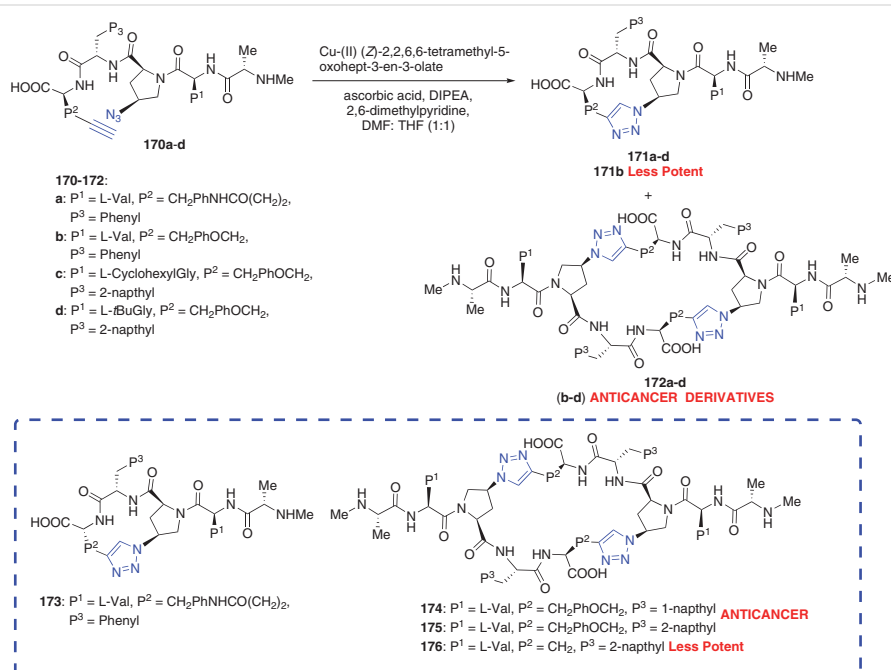
Scheme 17 Synthesis of apoptosis protein inhibitor **169**

drogenation furnished the desired dimeric macrocycle **169** in 57% yield. Biological assessment of **169** showed its binding ability to XIAP and cIAP proteins. The target compound also exhibited inhibition towards growth of human melanoma and colorectal cell lines by demonstrating prominent antitumor activity in the A875 human melanoma xenograft mode.

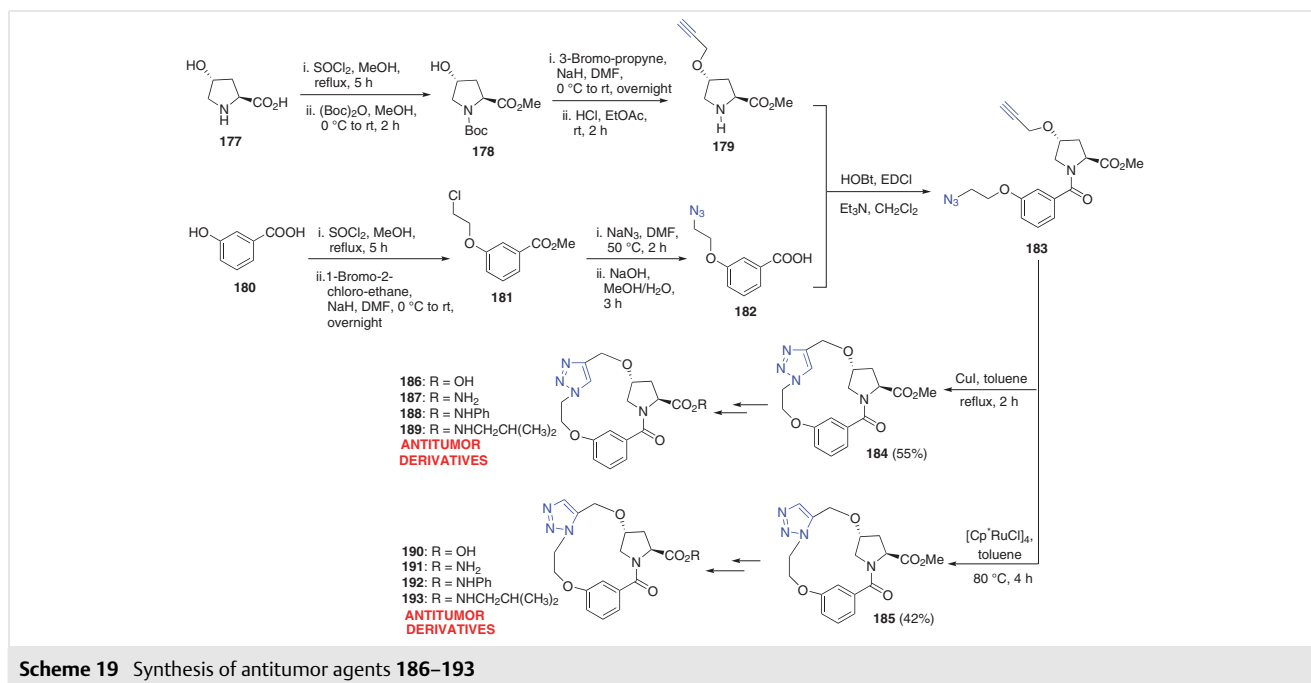
In 2015, Seigal *et al.* established a DNA-programmed library of cyclic peptidomimetics **171a–d**, **172a–d**, and **173–176** utilizing the Cu-catalyzed 1,3-dipolar cycloaddition reaction (Scheme 18).²⁶ The linear precursors were prepared on DNA solid-phase support using a reported DPC method. The crucial macrocyclization step took place by exposing the precursors **170a–d** to Cu(II) (*Z*)-2,2,6,6-tetramethyl-5-oxohept-3-en-3-olate, ascorbic acid, DIPEA and 2,6-dimethylpyridine in DMF/THF (1:1) solvent system, which provided the desired set of monomeric macrocycles **171a–d** after deprotection and resin cleavage with TFA. The dimers **172a–d** were simultaneously synthesized as a by-product of the aforementioned reaction but, their yields were increased by utilizing a higher substitution density in the solid-phase synthesis, which resulted in the enhancement of intermolecular cyclization. The monomeric macrocycle **173** was produced by inverting the P₂ linker in **170a** and exposing it to similar macrocyclization conditions, whereas the dimeric macrocycles **174–176** were produced by modifying all the P₁, P₂ and P₃ linkers. The macrocycles **171a** and **171b** were noted to bind potently to cIAP1 BIR3 and XIAP BIR3 in Fluorescence Polarization Assays (FPA), with IC₅₀ values around 3–8-fold lower in the case of the latter. Compound

171b showed less potency in the caspase-3 rescue assay, weak inhibition towards cell growth in human triple negative breast cancer type I MDA-MB-231 cell-lines, and no inhibition in type II A875 melanoma cell-lines. Dimer **172b** displayed an improved affinity against BIR2 and BIR3 when compared with its corresponding monomer **171b**. Macrocycle **172b** exhibited good caspase-3 rescue activity along with measurable antiproliferative activity in both type I and II cell lines, despite being potent towards the cIAP1 BIR3 domain. Dimer **172a** showed good binding towards the BIR domain and good caspase-3 rescue activity but no antiproliferation in either I or II cell-lines. Compound **173** had a slight effect on BIR3 affinity but a prominent reduction in BIR2 affinity. Macrocycles **174** and **175** portrayed prominent activity against type I cancer cell lines while showing sub-μM IC₅₀ values against type II A875 cells. Compounds **172c,d** were noted to exhibit low IC₅₀ values when evaluated against MDA-MB-231 cells and A875 cells, whereas compound **176** was found to display IC₅₀ values comparable to that of **172b**.

Cao *et al.*, in 2016, synthesized a set of triazole-fused macrocyclic derivatives **186–193** and investigated their antitumor activities (Scheme 19).²⁷ The synthetic procedure commenced with the conversion of carboxylic acid **177** into the Boc-protected ester **178** in two steps with further insertion of the alkyne group and subsequent Boc-deprotection to afford the synthon **179**. Next, the acid **180** was transformed into its corresponding ester **181** in two steps, which was followed by treatment with sodium azide and subsequent hydrolysis to afford the synthon **182**. The synthon



Scheme 18 Synthesis of a few macrocyclic anticancer agents



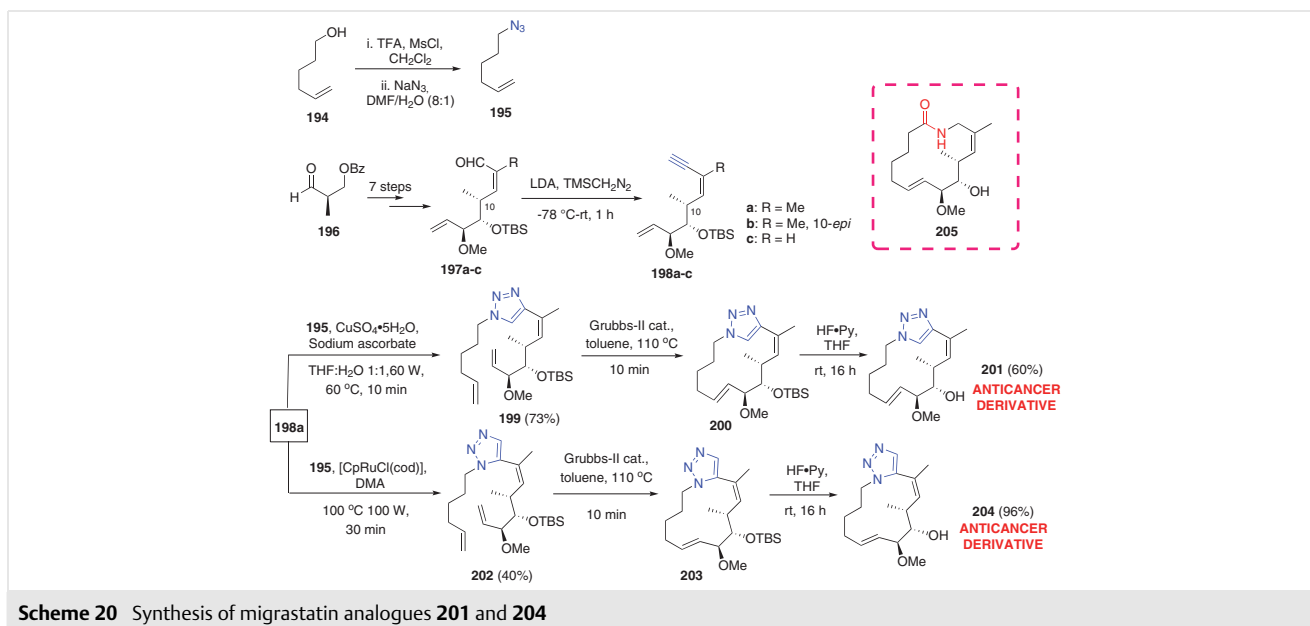
Scheme 19 Synthesis of antitumor agents **186–193**

179 was coupled with **182** to form the amide **183** under reaction conditions involving HOBt, EDCI with triethylamine in dichloromethane. On subjecting the macrocyclic precursor **183** to CuAAC reaction with CuI in refluxing toluene for 2 h, the 1,4-disubstituted triazole fused macrocycle **184** was achieved in 55% yield, whereas exposure to RuAAC reaction with catalytic $[\text{Cp}^*\text{RuCl}]_4$ in toluene at 80°C for 4 h, afforded the 1,5-disubstituted triazole-fused macrocycle **185** in 42% yield. Subsequently, the macrocyclic esters **184** and **185** were changed into their respective acid derivatives **186** and **190**, which were further made to undergo condensation with several amines to form the amide derivatives **187–189** and **191–193** in good yields. Biological evaluation of macrocycles **186–193** against lung cancer cell line A549, breast cancer cell line MDA-MB-231, and hepatocarcinoma cell line Hep G2 revealed moderate antitumor activity.

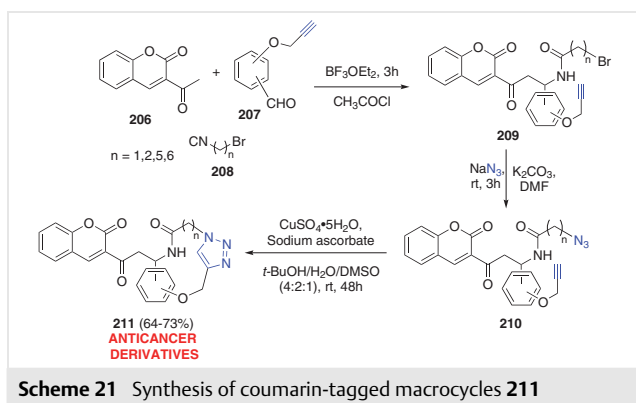
Migrastatin, an anti-metastatic agent originating from microbes, was isolated by Imoto and co-workers in 2000. In 2017, Gabba *et al.* synthesized the migrastatin-triazole derivatives **201** and **204** and evaluated their biological activities (Scheme 20).²⁸ In order to prepare the target macrocycles, the synthons **194** and **198a–c** were first synthesized. Activation of 5-hexen-1-ol **194** with methanesulfonyl chloride followed by treatment with sodium azide led to the formation of alkenylazide **195**. Preparation of synthons **198a–c** commenced with the use of aldehyde **196**; seven subsequent steps furnished the advanced intermediates **197a–c**, which were made to react in the presence of trimethylsilyl diazomethane and LDA to afford the required alkynes **198a–c**. Next, the azide-alkyne cycloaddition reaction was conducted upon the alkyne **198a** in two different

pathways. Initially, **198a** was coupled with the azide **195** in the presence of $\text{CuSO}_4 \cdot 5\text{H}_2\text{O}$ and sodium ascorbate in THF/water (1:1) medium under 10 min microwave irradiation (60 W) at 60°C to afford 1,4-disubstituted triazole derivative **199** (73%). The latter was further subjected to macrocyclization in presence of Grubbs' 2nd generation catalyst to furnish compound **200**, and subsequent removal of the TBS protecting group produced the desired compound **201** in 60% yield. A Ru-catalyzed azide-alkyne cycloaddition of **198a** and **195** was also conducted by Adele Gabba and her co-workers using catalytic $[\text{Cp}^*\text{Ru}(\text{cod})\text{Cl}]$ in DMA through 100 W irradiation at 100°C for 30 min to prepare the derivative **202** (40%). Exposure to metathesis conditions ensured the macrocyclization process and afforded the triazole-fused macrocycle **203**. Further deprotection of the TBS group yielded the second desired product **204** in 96% yield. Compounds **201** and **204** were biologically evaluated using the MDA-MB-361 cell line (human breast cancer) and were found to exhibit a significant effect to retard the process while being comparable to a well-known inhibitor of human tumor cell migrastatin **205**.

In 2017, Jithin Raj and Bahulayan developed a three-step multi-component coupling (MCR)-click strategy to synthesize a library of coumarin-tagged macrocycles **211** with ring-size ranging from 11 to 18 (Scheme 21).²⁹ The protocol commenced with an initial Mannich type reaction conducted with 3-acetyl coumarin **206**, alkyne **207**, and bromo nitriles **208** to afford the alkyne compounds **209**. Next, the azide group was introduced within the compound by treatment with sodium azide in DMF using potassium carbonate as a base. This action led to the formation of macrocycle

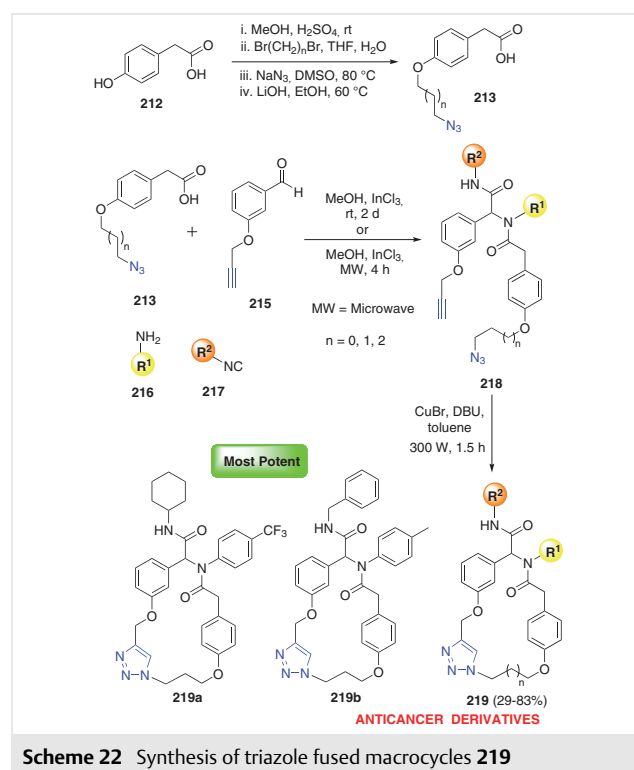


precursor **210**, which underwent intramolecular CuAAC reaction using copper sulfate and sodium ascorbate in the solvent system *t*-BuOH/H₂O/DMSO (4:2:1) for 48 h to afford the desired macrocycles **211** in 64–73% yields. The set of macrocycles were biologically evaluated and were found to show excellent cytotoxicity towards human breast cancer cell line (MCF-7), indicating them to be potential anticancer agents.



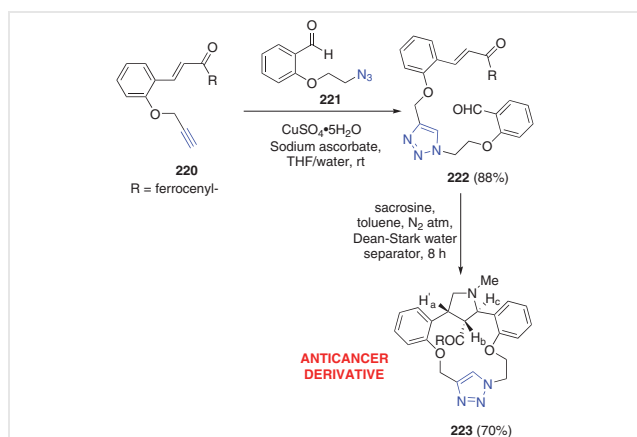
In 2018, Eduardo Hernandez-Vazquez and his co-workers reported the synthesis of a series of 20–22-membered triazole fused macrocycles **219** (Scheme 22).³⁰ They described a multicomponent approach that involved a Ugi four-component reaction (Ugi 4-CR) to assemble an acyclic precursor. Final macrocyclization was then carried out by intramolecular CuAAC reaction. The synthetic procedure commenced from the azido synthon **213**, which was prepared from *p*-hydroxyphenylacetic acid **212** in four consecutive steps and then treated with an aldehyde **215**, various

amines **216**, isonitriles **217**, and under Ugi 4-CR conditions to generate the acylamino carboxamides **218**. The Ugi adducts were next exposed to microwave radiation with Cu-Br/DBU in toluene for 1.5 h to ensure the formation of triazoles. Thus, macrocyclization led to the production of the triazole-fused compounds **219** in moderate to good yields



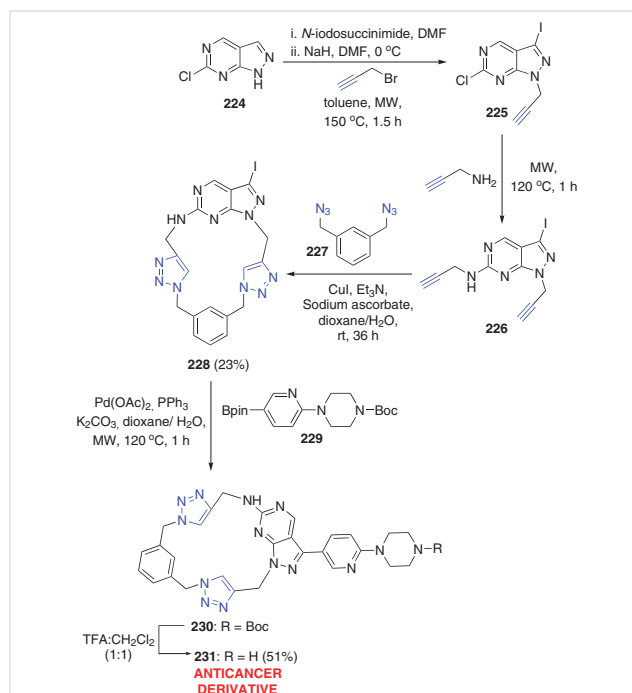
(29–83%). On being biologically evaluated, most compounds were seen to exhibit cytotoxicity against prostate (PC-3) and breast (MCF-7) cancer cells. IC₅₀ values of **219a,b** showed more than 50% PC-3 inhibition and **219a** also caused high levels of apoptosis in PC-3.

Prabhakaran *et al.*, in 2018, developed a synthetic route to synthesize a triazole-fused macrocycle **223** and evaluated its anticancer activity (Scheme 23).⁷ The synthesis proceeded with the intermolecular click-reaction between alkyne **220** and azide **221** in the presence of copper sulfate and sodium ascorbate, in THF/H₂O medium at room temperature. This afforded the triazole-based macrocyclic precursor **222** in 88% yield, which was subsequently subjected to reflux in toluene with sarcosine in a Dean–Stark apparatus to provide the target macrocycle **223** (70%). Biological investigation showed that **223** displayed prominent anticancer activity against human adenocarcinoma breast cancer cell lines MCF-7.



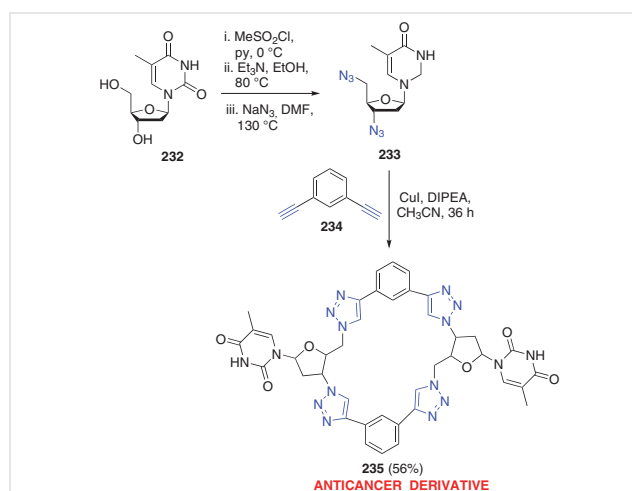
Scheme 23 Synthesis of triazole-fused macrocycle **223**

In 2019, Cruz-Lopez *et al.* constructed an 18-membered triazole-fused macrocycle **231** through double CuAAC reaction (Scheme 24).³¹ The synthetic pathway commenced as the commercially available 6-chloro-1*H*-pyrazolo[3,4-*d*]pyrimidine **224** was iodinated with *N*-iodosuccinimide followed by propargylation with propargyl bromide to afford the intermediate **225**. Subsequent steps ensured the introduction of a second alkyne group within the moiety and led to the development of dialkyne compound **226**, which was further assembled with 1,3-bis(azidomethyl)benzene **227** in the presence of copper iodide, sodium ascorbate, and triethylamine in dioxane/H₂O medium at room temperature for 36 h to achieve the macrocycle **228** (23%). The desired macrocyclic compound **231**, analogue of multikinase inhibitor eSM119, was obtained in 51% yield when **228** was cross-coupled with 6-(4-Boc-piperazinyl)pyridyl-3-boronic acid pinacol ester **229** and Boc-protected under acidic conditions. The desired compound **231** was found to display selective inhibitory activity against the receptor tyrosine kinase AXL.

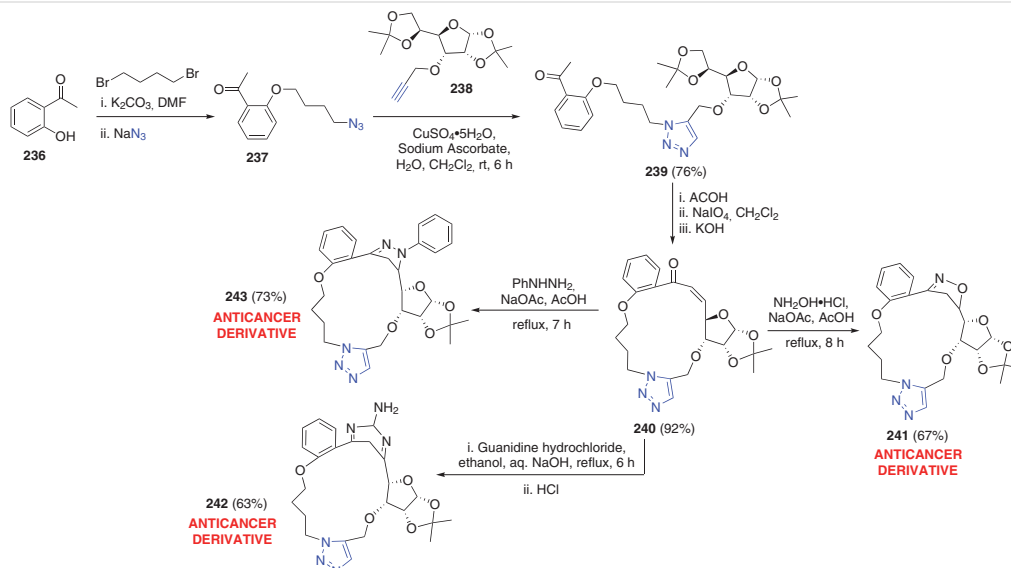


Scheme 24 Synthesis of triazole-fused macrocycle **231**

Rahman *et al.*, in 2020, developed a thymidine analogue with linked triazoles **235** and tested its anti-proliferative activities (Scheme 25).³² Commercially available thymidine **232** was initially converted into its di-azide derivative **233** in three sequential steps and subsequently exposed to CuAAC reaction with 1,3-diethynyl benzene **234** using a CuI/DIPEA system in acetonitrile for 36 h to afford the macrocyclic thymidine analogue **235** (56%). Biological assessment showed that **235** expressed significant toxicity when tested against C6 glioblastoma cancer cell lines, MCF7



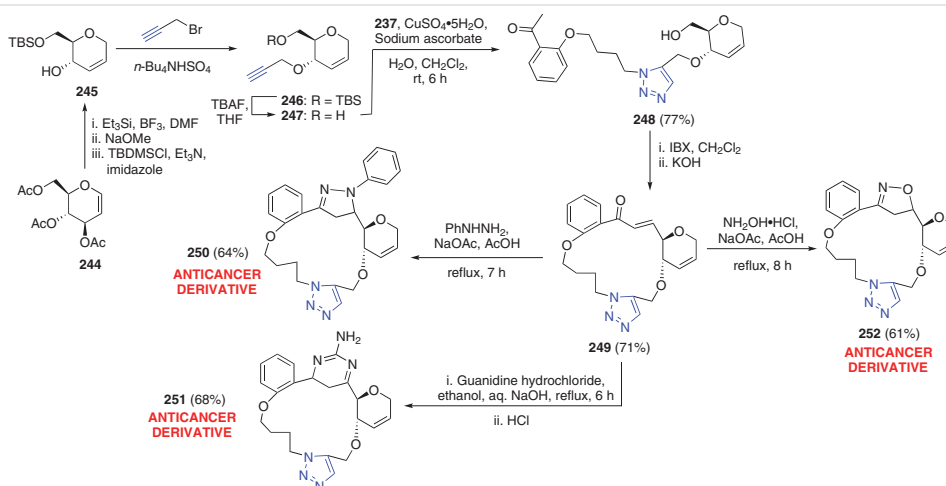
Scheme 25 Synthesis of thymidine analogue **235**

Scheme 26 Synthesis of anticancer agents **241–243**

breast cancer cell lines and HT29 colorectal adenocarcinoma cell lines.

In 2021, Srinivas and Rao reported a series of triazole-fused macrocycles **241–243** and **250–252** and assessed their anticancer activity (Scheme 26 and Scheme 27).³³ They implemented their idea by using 1-(2-hydroxyphenyl)ethan-1-one **236** as their starting material (Scheme 26). Compound **236** was converted into azide **237** by the consecutive action of 1,4-dibromopropane and sodium azide. Subsequently, **237** was subjected to cycloaddition reaction with **238** using copper sulfate and sodium ascorbate in a dichloromethane/water solvent system to afford triazole **239** in 76% yield. Three steps were then followed to furnish the triazole-fused macrocycle **240** in 92% yield. Finally, com-

pound **240** was heated at reflux using three different core reagents viz. hydroxylamine, hydrazine hydrochloride and guanidine hydrochloride to achieve the target macrocycles **241** (67%), **242** (63%) and **243** (73%). Another set of macrocycles were prepared using **244** as the starting material (Scheme 27). After subjecting **244** to three reaction steps, the TBS-protected compound **245** was achieved, which was further propargylated to create the alkyne moiety **246**. Deprotection of the TBS group resulted in the formation of **247**, which, upon exposure to azide-alkyne cycloaddition reaction conditions with **237**, furnished triazole **248** in 77% yield. Two subsequent steps helped graft the intermediate **249** (70.58%). The latter was allowed to react in three different pathways to afford the target macrocycles **250** (64%),

Scheme 27 Synthesis of anticancer agents **250–252**

251 (68%) and **252** (61%) by following a similar methodology described earlier. Biological evaluation of these compounds showed promising anticancer activity of **241** and **252** against MCF-7 cell line, whereas compounds **242**, **243**, **250** and **251** were noted to exhibit activity against MDA-MB-231 and HeLa cell lines.

In 2021, Vazquez-Miranda and co-workers extended their previous synthesis of triazole-fused macrocycles **258** and explored the anticancer activity of the reported compounds (Scheme 28).³⁴ Through the Ugi four-component reaction, amines **253**, isonitriles **254**, azides **255** and the alkyne moiety **256** were made to react together using a catalytic amount of InCl_3 in methanol to afford a set of macrocyclic precursors **257**. The final macrocyclization was conducted via CuAAC reaction, in the presence of CuBr and DBU in toluene under microwave irradiation, to afford the desired set of compounds **258** in 25–79% yields. The newly synthesized cyclophanes were biologically evaluated against prostate (PC-3 and DU-145) and breast (MCF-7) tumour cells and were reported to exhibit significant cytotoxicity. Compound **259** (Figure 1) was reported to induce apoptosis in PC-3 in their previous work³⁰ and was treated as a reference for this work. Compound **258a** was noted to display a two-fold higher inhibition towards PC-3 compared with **259**, and a lower toxicity towards healthy line COS-7. The derivative **258b** was also noted to be one of the most biologically active compounds from the entire set. From all of the observations noted, the Hernandez-Vazquez group concluded that the higher activity could be attributed to the presence of cyclohexyl and 4-isopropylaniline groups.

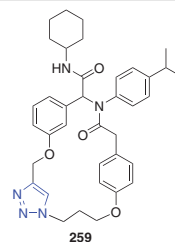
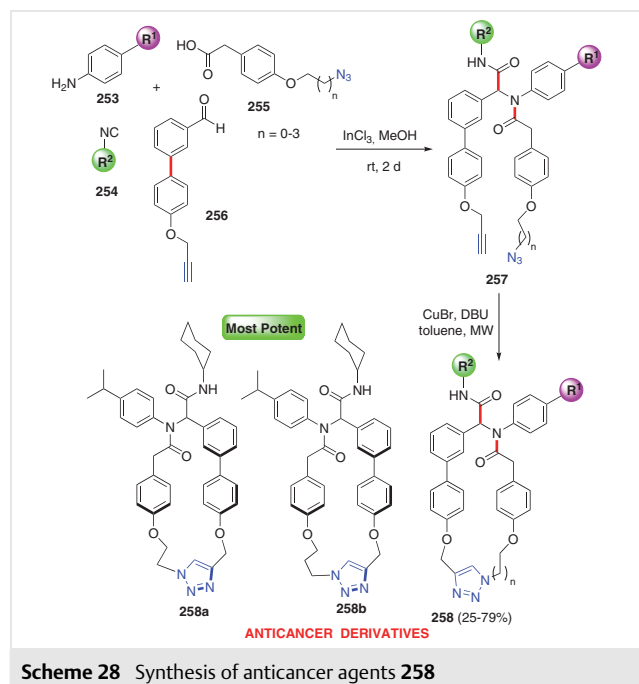
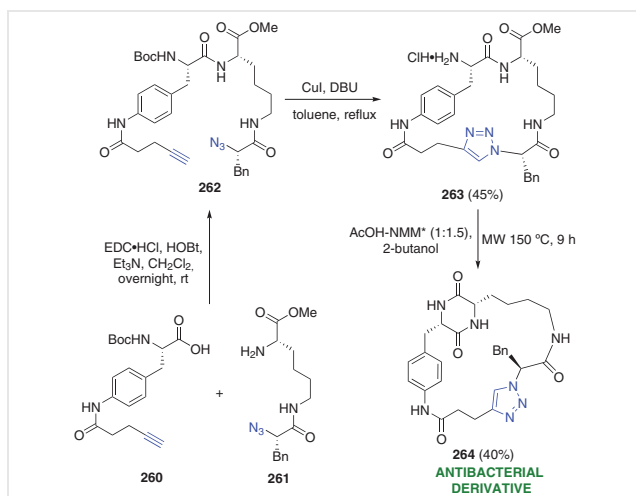


Figure 1 Macrocycle **259** for potency comparison of **258**

3 Antibacterial Derivatives

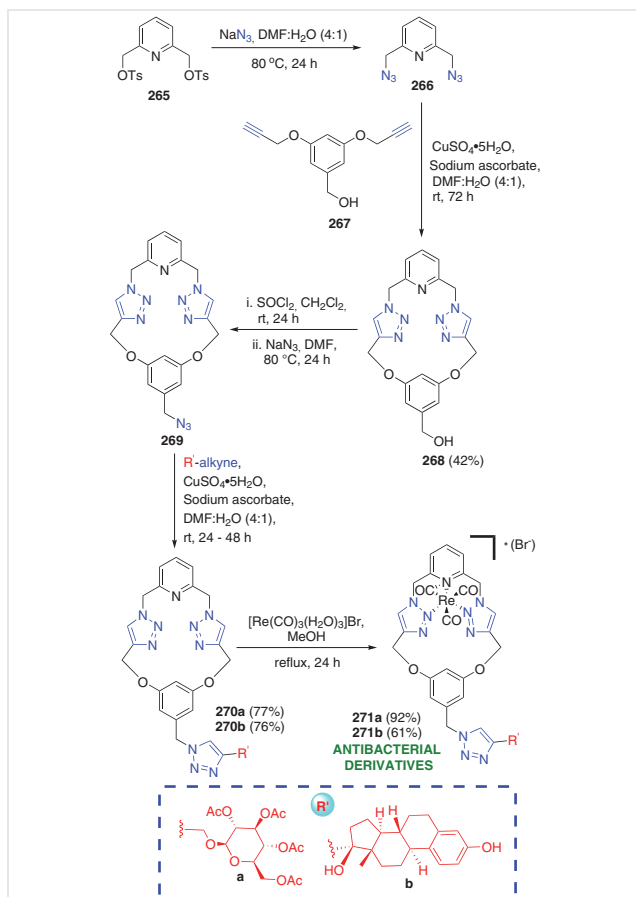
Antibiotic resistance, another global threat, has been an important research scope for scientists. Significant progress has been made so far in this field to treat bacterial infections. Many bioactive molecules are known to have the smallest cyclic peptides, diketopiperazines (DKPs), within their frameworks. Peptide or peptidometric incorporated macrocycles can modulate biological systems and are thus extremely important in the medicinal chemistry field. Isidro-Llobet *et al.*, in 2011, synthesized macrocyclic peptidometric framework **264**, the structure of which was inspired by a bioactive molecule (+)-piperzainomycin (Scheme 29).³⁵ Amide coupling in between the alkyne moiety **260** and azide **261** using EDC and HOBt led to the production of the macrocyclic precursor **262**. Subsequently, the latter was subjected to CuAAC conditions with catalytic CuI and DBU in refluxing toluene to afford the triazole-fused macrocycle **263** in 45% yield. The final DKP formation was achieved using solid-supported NMM under microwave heating at 150 °C for 9 h to furnish the target compound **264** in 40% yield. Biological assessment showed that the target macrocycle **264** exhibited prominent antibacterial property against the Gram-positive bacteria *Staphylococcus aureus*.

Noor *et al.*, in 2014, reported the development of a set of triazole-fused macrocycles that formed stable $[\text{Re}(\text{CO})_3]^+$ complexes **271a,b** and evaluated their antibacterial activities (Scheme 30).³⁶ The synthetic procedure progressed with the conversion of the tosylated derivative **265** into the 2,6-bis(azidomethyl)pyridine **266** by the action of sodium azide in DMF/ H_2O at 80 °C for 24 h. The azide moiety was then treated with dialkyne **267** in the presence of copper sulfate and sodium ascorbate in DMF/ H_2O (4:1) medium at room temperature for 72 h to afford macrocycle **268** in 42% yield. The latter was further converted into **269** in two reaction steps, which was subsequently exposed to another intermolecular Cu-catalyzed cycloaddition with two alkynes, under reaction conditions similar to those described earlier, to furnish compounds **270a,b** (77%, 76%). Subsequently, the rhenium(I) complexes **271a,b** were prepared in 92% and 61% yields by refluxing **270a,b** in methanol with $[\text{Re}(\text{CO})_3(\text{H}_2\text{O})_3]\text{Br}$ for 24 h. Biological evaluation helped in

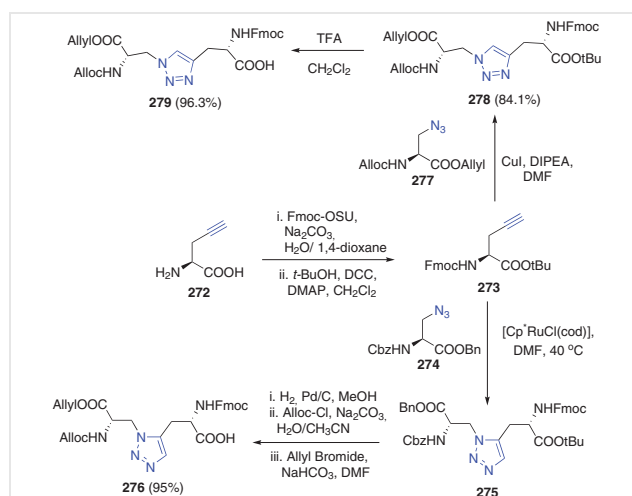


Scheme 29 Synthesis of macrocyclic peptidometric framework **264**

detection of the inhibitory activity of compounds **271a,b** against bacterial strains *Staphylococcus aureus* and *Escherichia coli*.

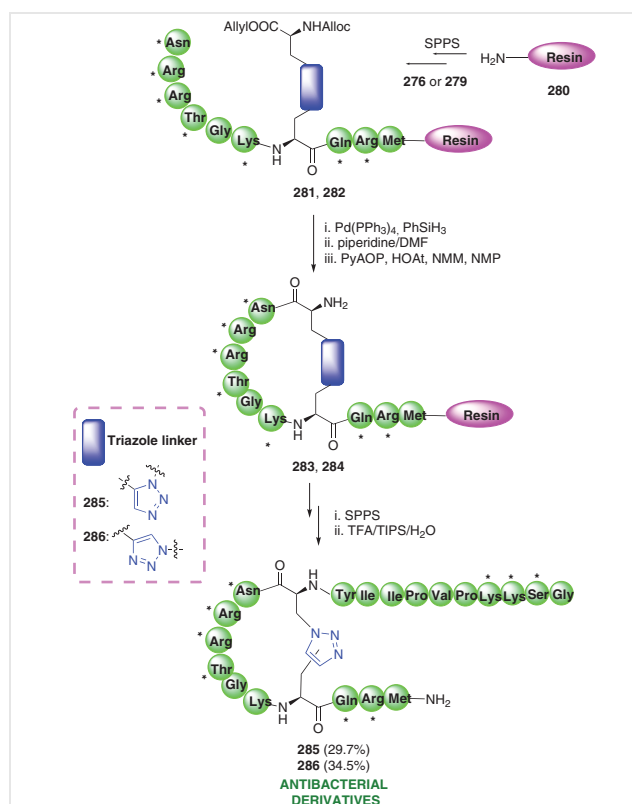


Scheme 30 Synthesis of antibacterial agents of Re-complexes **271a,b**



Scheme 31 Synthesis of triazole fragments **276, 279** required for **285, 286**

Guo *et al.*, in 2017, constructed the thanatin derived 1,2,3-triazole bridged disulfide surrogated peptides **285, 286** and tested their antibacterial activities (Scheme 31 and Scheme 32).³⁷ The process commenced by installing the *t*-butyl group, followed by Fmoc protection on 2-propargyl-Lglycine **272** to afford the fragment **273**, which was clicked



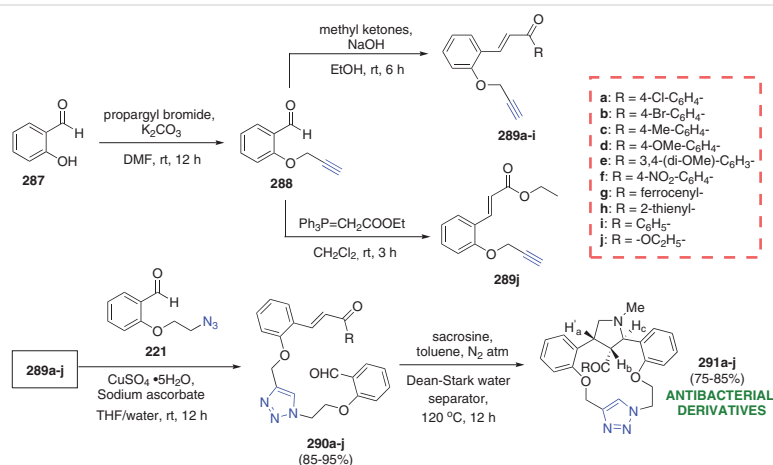
Scheme 32 Synthesis of antibacterial peptide macrocycles **285, 286**

with azide **274** via $[\text{Cp}^*\text{RuCl}(\text{cod})]$ catalyzed reaction in DMF at 40 °C to form the triazole moiety **275**. Three subsequent reactions led to the production of a key fragment **276** in 95% yield. In a separate pathway, **273** was coupled with azide **277** in the presence of the CuI/DIPEA system in DMF and the triazole **278** was furnished in 84.1% yield. TFA-mediated deprotection of **278** produced the second key fragment **279** in 96.3% yield. The peptidomimetics **285** and **286** were synthesized from the Rink amide AM resin by suitable assembly of Fmoc/*t*-Bu SPPS, using the coupling reagent HCTU, to create the macrocyclic precursors **281**, **282**. Successful cleavage of the allyl and Alloc groups with $[\text{Pd}(\text{PPh}_3)_4]/\text{PhSiH}_3$ was followed by cyclization with PyAOP, NMM and HOAt to graft the cyclic peptides **283**, **284**. After the remaining amino acids were united, deprotection and acidic cleavage afforded the compounds **285** and **286** in 29.7% and 34.5 yields, respectively. Through biological assessment, it was realized that both of the 1,5- and 1,4-disubstituted triazole peptides showed 50% less inhibition against *Pseudomonas aeruginosa* compared with thanatin.

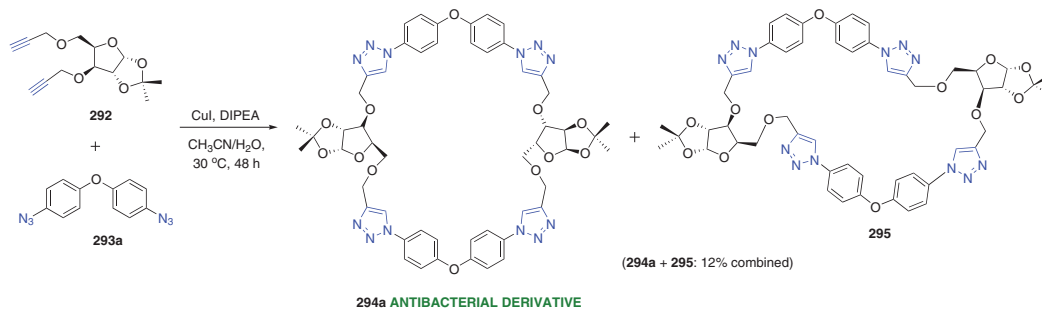
Prabhakaran *et al.*, in 2018, developed a synthetic route to synthesize triazole-fused macrocycles **291a–j** and then evaluated their bioactivities (Scheme 33).⁷ The synthesis in-

involved propargylation of salicylaldehyde **287** to afford the derivative **288** followed by aldol condensation with various methyl ketones to achieve the unsaturated ketones **289a–i**. In addition, the only unsaturated ester **289j** was synthesized *via* Wittig reaction of **288**. Subsequently, intermolecular cycloaddition of **289a–j** with *O*-alkylazidoaldehyde **221** in the presence of copper sulfate and sodium ascorbate in THF/H₂O (1:1) at room temperature for 12 h furnished the 1,2,3-triazole-linked moieties **290a–j** in 85–95% yields. Final cyclization of the aldehydes **290a–j** with sarcosine in toluene at 120 °C for 12 h afforded the desired macrocycles **291a–j** in 75–85% yields. Several biological assessments conducted on **291a–j** concluded that these macrocycles showed significant antibacterial activity against *Bacillus cereus* and *Klebsiella pneumoniae*.

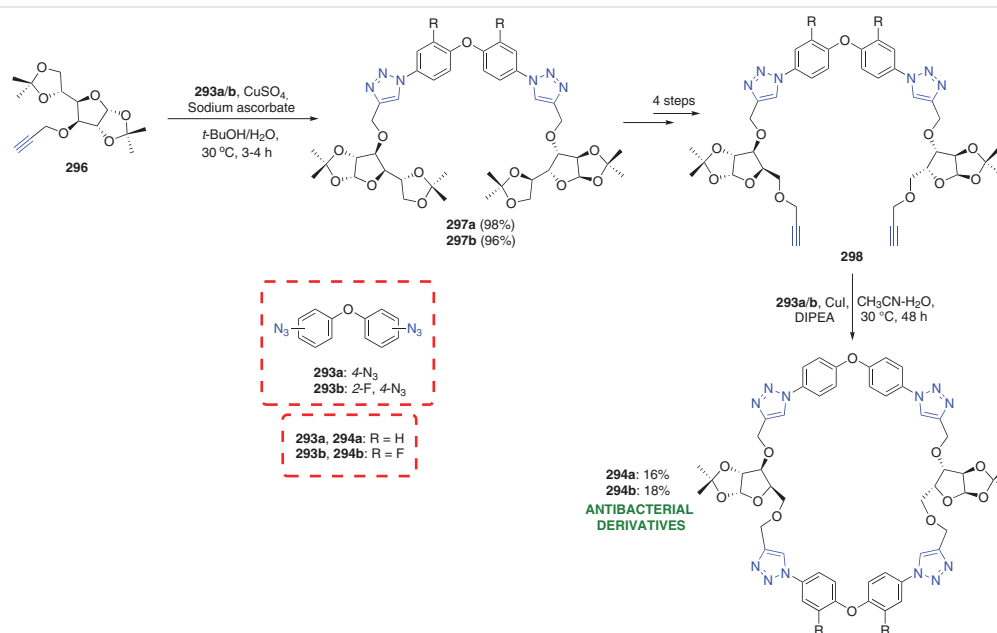
Biaryl ethers have always been an interesting scaffold for researchers because they possess various bioactivities. In 2018, Singh *et al.* developed vancomycin-like 44-membered biphenyl ether based macrocycles with triazole linkers **294a,b** and evaluated their antibacterial activities (Scheme 34 and Scheme 35).³⁸ Their syntheses were undertaken by using the azido-biphenyls **293a** and **293b** along with the propargylated sugar moieties **292** and **296**. The



Scheme 33 Synthesis of antibacterial agents **291a–j**

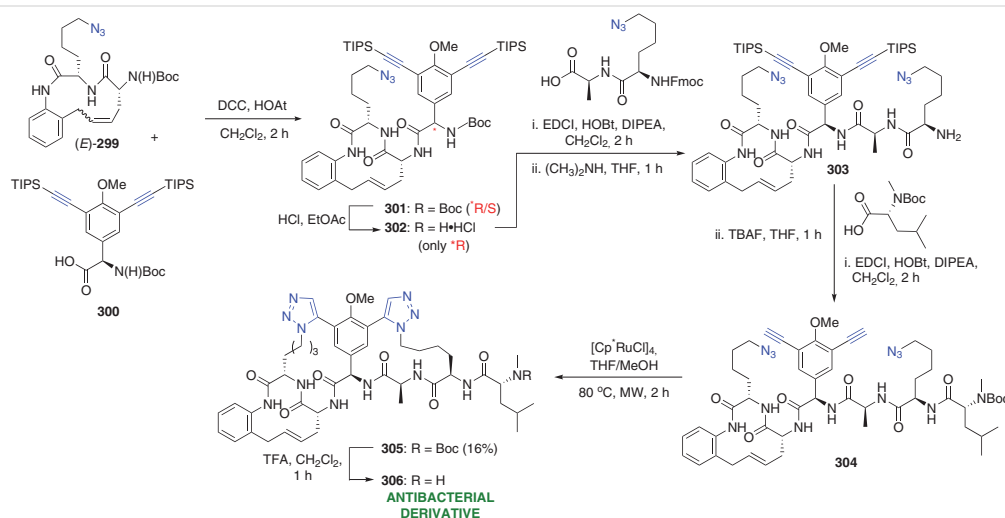


Scheme 34 Synthesis of antibacterial agent **294a**

Scheme 35 Synthesis of antibacterial agents **294a,b**

initial Cu-catalyzed AAC reaction conducted between **293a** and **292** in the CuI/DIPEA system in acetonitrile/water medium at 30 °C for 48 h afforded the target macrocycle **294a** and its isomer **295** as an inseparable mixture with a combined yield 12% (Scheme 34). Thus, in order to selectively afford the target compound, the substrate **296** was clicked with the triazides **293a** and **293b**, respectively, in the presence of copper sulfate and sodium ascorbate in *t*-BuOH/water medium at 30 °C for 3–4 h. This afforded the key intermediates **297a,b** in excellent yields of 98% and 96%, respectively (Scheme 35). Two subsequent steps led to the

formation of the dialkyne **298**, which was finally subjected to CuAAC reaction with azides **293a/293b** in the CuI/DIPEA system under reaction conditions similar to those described earlier. This afforded the desired triazole fused macrocyclic compounds **294a** and **294b** in 16% and 18% yields, respectively. Through biological investigation, it was reported that both of the compounds exhibited antibacterial activity against *Staphylococcus aureus*. It was noted that the fluoro substituted compound **294b** displayed significant activity against both Methicillin-resistant SA and Vancomycin-resistant SA strains.

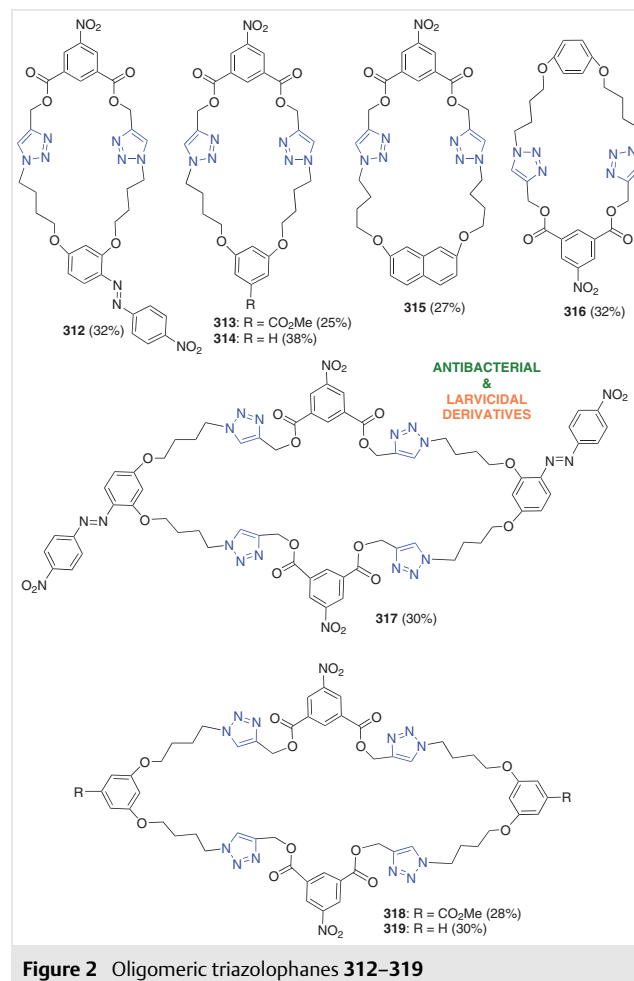
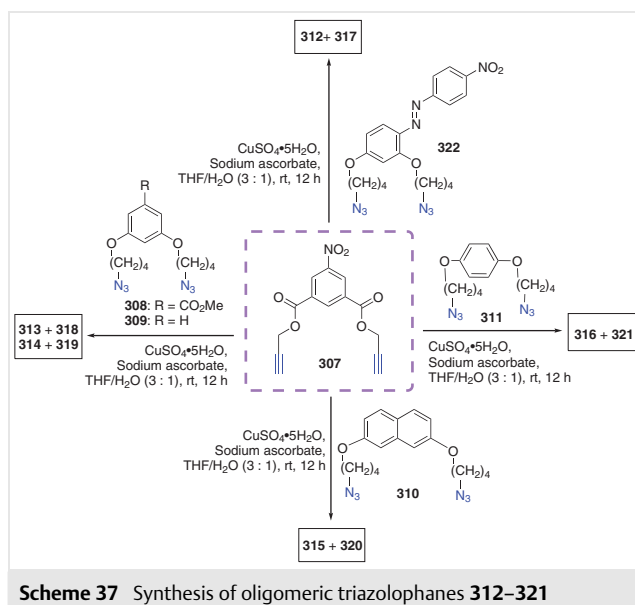
Scheme 36 Synthesis of tricyclic hexapeptide **306**

In 2022, the Liskamp group constructed a tricyclic hexapeptide **306** that mimicked the topology of a potent antibiotic vancomycin (Scheme 36).³⁹ The process was initiated with coupling of the amine (*E*)-**299** and the acid fragment **300** under DCC/HOAt conditions in dichloromethane to achieve the amide **301**. After acidic treatment of **301**, Boc deprotection resulted in the formation of **302**, which was further converted into the macrocyclic precursor **304** in four consecutive reactions. Subsequently, the crucial intramolecular macrocyclization step was conducted using [Cp*RuCl]₄ catalyst in THF/MeOH (4:1) medium at 80 °C under microwave irradiation for 2 h to furnish the tricyclic compound **305** in 16% yield. Finally, Boc deprotection with acid yielded the target compound **306**, which displayed significant antibacterial activity against *Staphylococcus aureus*.

4 Derivatives with Dual Activity

Research on the synthesis of macrocyclic compounds has led to the development of certain compounds that exhibit dual bioactivities. Selvarani *et al.*, in 2018, synthesized a series of 1:1 and 2:2 oligomeric triazolophanes **312–321** and evaluated their antibacterial activities (Scheme 37, Figure 2 and Figure 3).⁴⁰ The synthetic process advanced with the preparation of bispropargyl-5-nitroisophthalate **307** and the respective bisazides **322**, **308–311**. The building block **307** was obtained by propargylating 5-nitroisophthaloyl chloride, whereas the bisazides were synthesized using 1,4-dibromobutane and various diols as the starting materials. For the crucial macrocyclization step, the fragment **307** was coupled with each of the bisazides (**322**, **308–311**) using a catalytic amount of copper sulfate and sodium ascorbate in THF/H₂O (3:1) solvent system at room tem-

perature for 12 h (Scheme 37). The 1:1 triazolophanes (**312–316**) were obtained in 25–38% yields, whereas the 2:2 triazolophanes **317–321** were received in 25–30% yields through the advancement of the CuAAC reaction (Figure 2, Figure 3). Biological screening of the synthesized triazole-fused macrocycles **312–321** was conducted with four bacterial strains viz. *Staphylococcus aureus* (MTCC96), *Bacillus subtilis* (MTCC441), *Salmonella typhi* (ATCC 6539) and *Escherichia coli* (MTCC 1698). When tested against the standard tetracycline, all the compounds showed significant inhibition, with compounds **312** and **314** exhibiting a greater zone of inhibition compared with **312**, **313** and **315**. Macrocyclic **317** was seen to display a stronger inhibition towards the Gram-positive bacteria *S. aureus* and *B. subtilis* than the Gram-negative bacteria *E. coli* and *S. typhi*. Further, molecular docking studies via Glide XP established the binding ability of macrocycles **313–316** with the target protein CTXM-enzyme in complex with cefotaxime. Selvarani *et al.* also investigated the bioactivities of **312–321** against the larvae of vector *Aedes aegypti*. The compounds shown in Figure 2 and Figure 3 exhibited larvicidal activity, with 90% mortality rate in the case of **316**. Macrocycles **314** and **315**



were reported to display 80% mortality rate whereas **312–313** showed moderate rate and **317–321** showed low mortality.

5 Antilarval Derivatives

The cowpea aphid or *Aphis craccivora* Koch has been a major problem for agriculture because it affects the growth of leguminous crops by sucking the sap from leaves and transmits viruses, which ultimately causes economic damage. Researchers are investing efforts to eradicate these pests by developing new macrocyclic drugs to help vegetation flourish.

In 2017, Rana and co-workers reported the synthesis of a few triazole-fused sugar-embedded macrocycles **326**, **329**, **333** and presented their bioactivities in 2018 (Scheme 38).^{10,41} The synthetic process was carried out with the preparation of the macrocyclic precursors **325**, **328** and **332**. The alkyne moiety **323** and the azide moiety **324** were exposed to CuI-catalyzed AAC reaction in water at 70 °C for 2 h to achieve the intermolecular click product **325** in 78% yield. Subsequently, ring-closing metathesis (RCM) reaction was conducted upon **325** in the presence of Grubbs-II catalyst in two different pathways with varying amount of catalyst added in the reaction mixtures. For method A, the substrate was heated at reflux in dichloromethane for 3 h, which afforded the triazole fused macrocycle **326** in 83% yield. Simultaneously, for method B, the substrate was heated at 75 °C in ethyl acetate for 2 h and the desired macrocycle **326** was grafted in 39% yield. The fragments **327** and

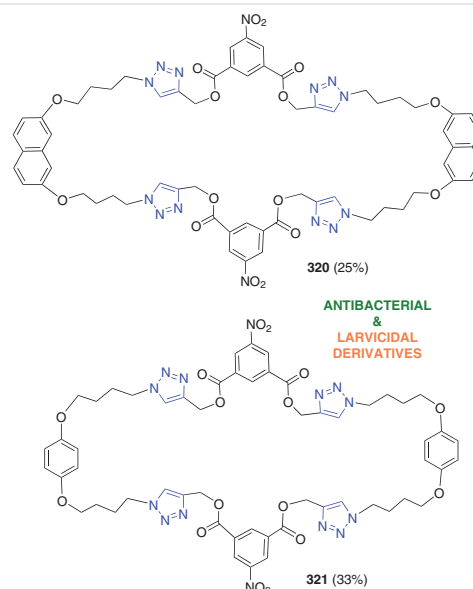
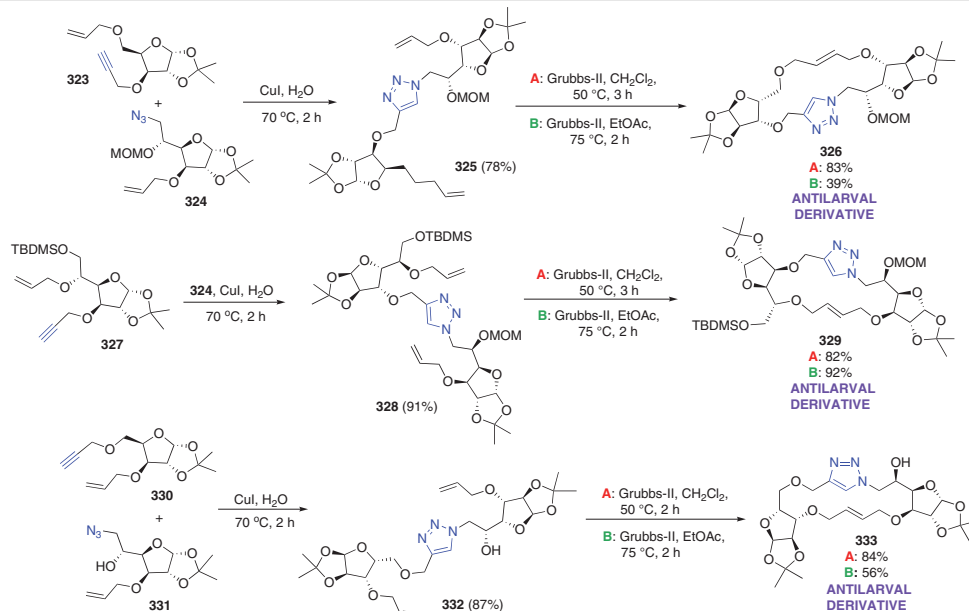
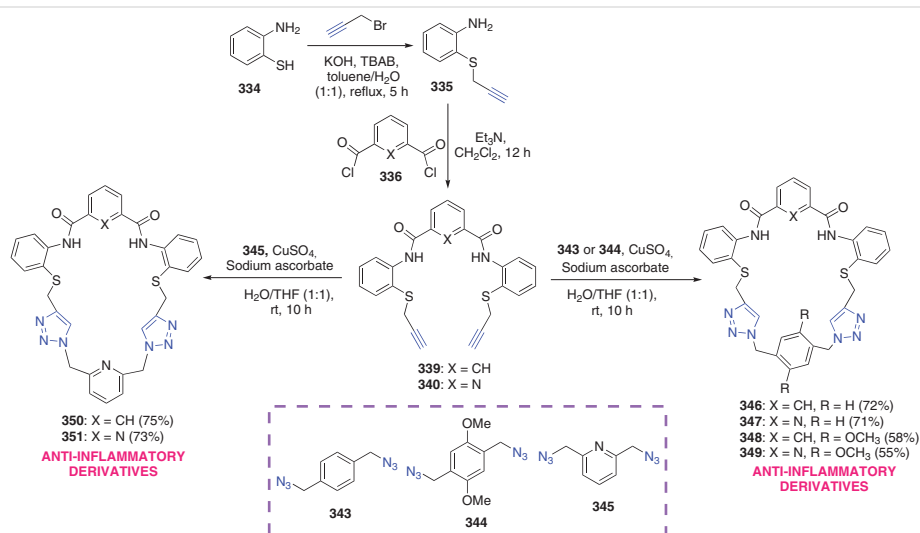


Figure 3 Oligomeric triazolophanes **320**, **321**

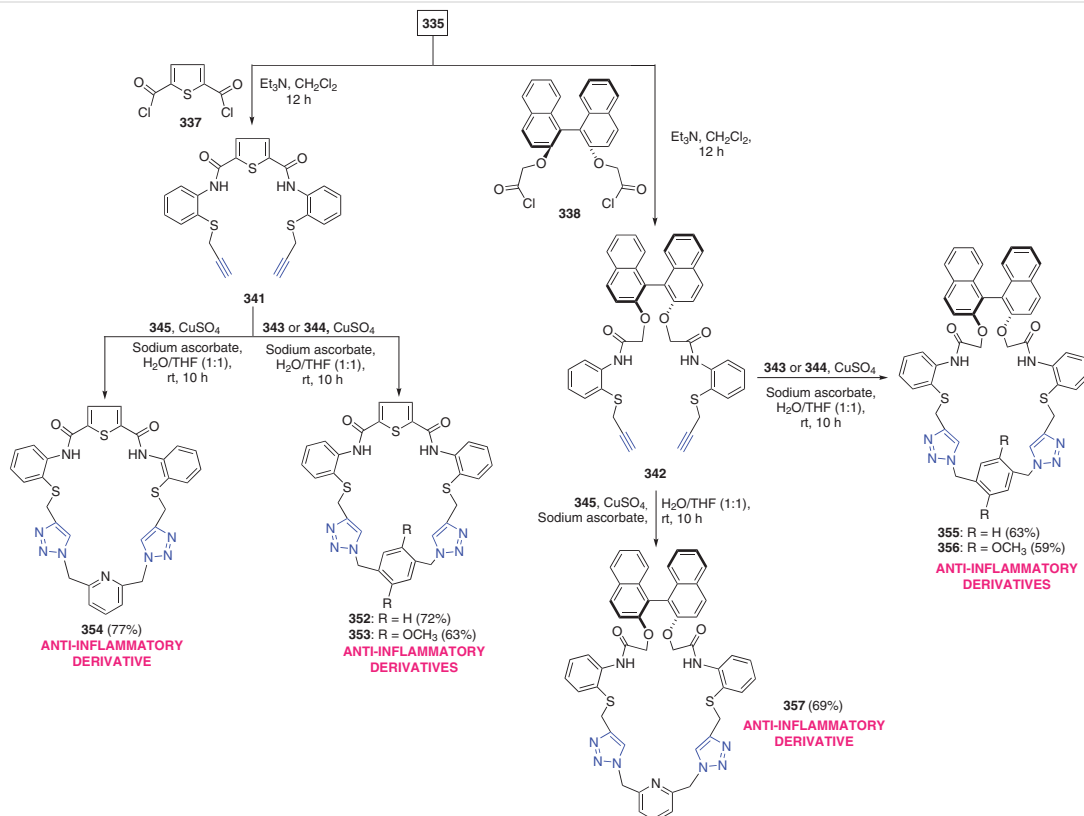
324 were coupled under similar CuAAC reaction conditions to synthesize the macrocyclic precursor **328** (91%), which was further subjected to two different RCM reactions following the conditions mentioned earlier. The target macrocycle **329** was afforded in yields of 82% (method A) and 92% (method B), respectively. Compounds **330** and **331** were clicked together to afford **332** (87%), which underwent macrocyclization via RCM and formed the desired com-



Scheme 38 Synthesis of antilarval sugar-embedded macrocycles **326**, **329** and **333**



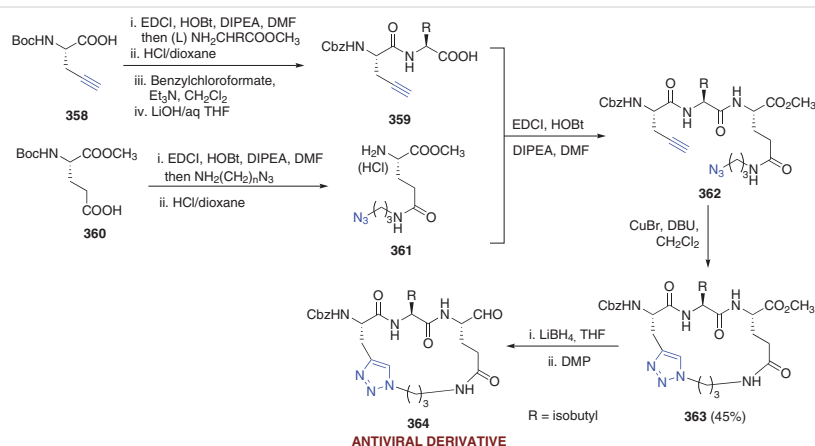
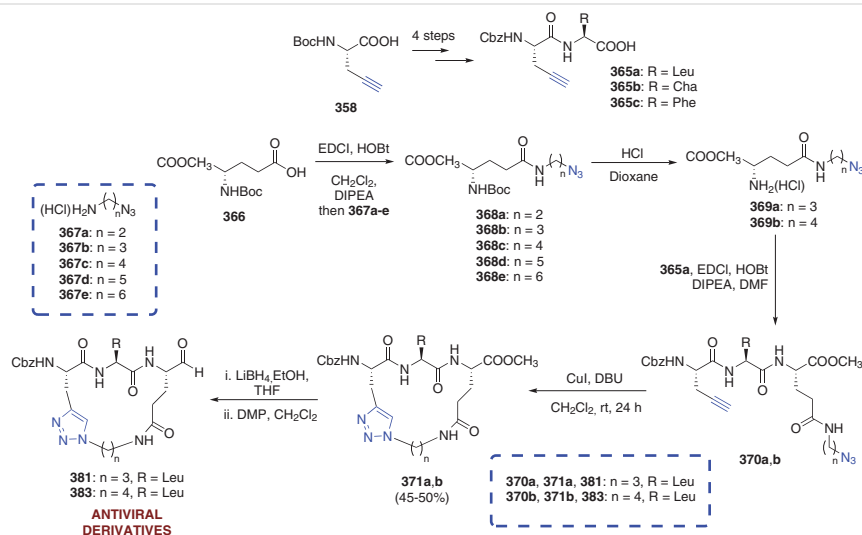
Scheme 39 Synthesis of macrocycles **346–351** with anti-inflammatory activity



Scheme 40 Synthesis of macrocycles **352–357** with anti-inflammatory activity

pound **333** in yields of 84% (method A) and 56% (method B). Biological screening of these macrocycles was conducted to evaluate their toxicity against larvae of *Aphis craccivora* Koch. Compound **328** was seen to exhibit the highest toxic-

ity (93.33%) against the larvae, compound **326** showed prominent toxicity (83.33%), whereas compound **333** displayed 73.33% toxicity.

Scheme 41 Synthesis of antiviral agent **364**Scheme 42 Synthesis of antiviral agents **381**, **383**

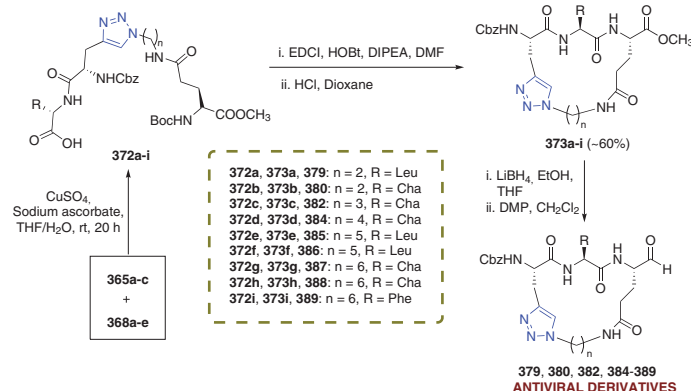
6 Anti-inflammatory Derivatives

In order to reduce inflammation caused by various health issues, particularly arthritis, a focus of attention has been the development of few 'clickable' cyclophanes. In 2016, Anandhan *et al.* synthesized and screened the anti-inflammatory activity of certain triazole-based macrocycles (Scheme 39 and Scheme 40).⁸ The synthetic procedure commenced with propargylation of the amine **334** using KOH and TBAP in a toluene/H₂O solvent system to afford the alkyne moiety **335**. Compound **335** was subjected to three different reaction pathways to afford the macrocyclic precursors **339**–**342**, which were subsequently made to react with the azides **343**–**345** by following the cycloaddition reaction methodology using copper sulfate and sodium ascorbate in THF/H₂O medium at room temperature for 10 h in

order to furnish a set of triazole-based macrocyclic compounds **346**–**357** (55–77%). All the macrocycles exhibited good anti-inflammatory activity when compared to the reference prednisolone.

7 Antiviral Derivatives

Viral infections have always been affecting the lives of people and are an important health concern. In order to combat with such infectious diseases, researchers have paid significant attention to the development of drugs required for treatment. In 2013, Mandadapu *et al.* reported the synthesis and bioevaluation of macrocyclic inhibitor **364** of 3C and 3C-like proteases of viral pathogens (Scheme 41).⁹ The synthetic procedure advanced with the development of the



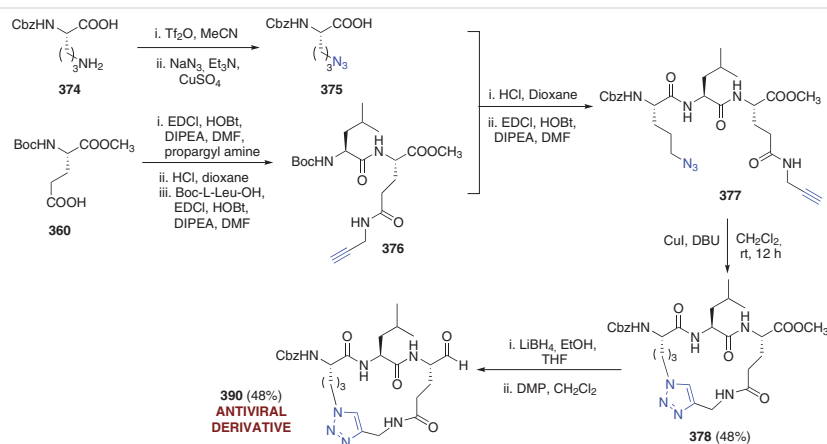
Scheme 43 Synthesis of some antiviral agents

building block **359** from the (L) Boc-protected propargyl glycine **358** in four consecutive steps while the second building block **361** was synthesized from commercially available (L) Boc-Glu-OCH₃ **360** in two steps. These two were gradually coupled under standard conditions using HOBt and EDCI with DIPEA in DMF to graft the amide **362**, which was further subjected to cycloaddition reaction conditions using CuBr, DBU in dichloromethane to afford the triazole-fused macrocycle **363** in 45% yield. Further treatment of **363** with lithium borohydride converted it into an alcohol, which subsequently formed the desired macrocycle **364** through Dess–Martin periodinane oxidation. Through biological assessment, compound **364** was noted to exhibit inhibition against novovirus 3CLpro, enterovirus 3Cpro and SARS-CoV 3CLpro.

Weerawarna *et al.*, in 2016, developed a series of triazole-fused macrocycles **379–390** and evaluated their antiviral properties (Scheme 42, Scheme 43 and Scheme 44).⁴² The synthesis progressed with the construction of the key intermediates **365a–c**, **368a–e** and **369a,b**. Initially, the commercially available *N*-Boc-protected L-propargylglycine

358 was transformed into the intermediates **365a–c** in four consecutive steps. A subsequent coupling of *N*-Boc protected glutamic acid **366** and HCl salts of amino azides **367a–e**, under standard conditions involving EDCI and HOBt, proceeded to furnish the intermediates **368a–e** (Scheme 42). Deprotection of the Boc-group in the presence of HCl yielded the azides **369a,b**, which further underwent coupling with acid **365a** in the presence of EDCI and HOBt to afford the macrocyclic precursors **370a,b**, respectively. The crucial macrocyclization step was then undertaken *via* intramolecular CuAAC reaction in the presence of CuI with DBU in DCM solvent at room temperature for 24 h to achieve the macrocycles **371a,b** in 45% and 50% yields. Sequential reduction with LiBH₄ and oxidation through Dess–Martin periodinane afforded the desired triazole-based macrocycles **381** and **383** in good yields (Scheme 42).

In order to synthesize the other macrocycles **379**, **380**, **382**, and **384–389**, the key intermediates **365a–c** and **368a–e** were coupled in the presence of copper sulfate and sodium ascorbate in THF/H₂O at room temperature for 20 h to graft the triazole linked fragments **372a–i** (Scheme 43).



Scheme 44 Synthesis of antiviral agent 390

Subsequent amide bond formation through acid-amine coupling with a sequenced Boc-deprotection constructed the macrocycles **373a–i** in fair yields (ca. 60%). A similar reaction methodology of consecutive reduction-oxidation upon **373a–i** resulted in the formation of the desired macrocyclic compounds **379**, **380**, **382**, and **384–389**.

The synthesis of the last macrocycle **390** commenced with the reaction of (*Z*)-L-ornithine with triflic azide solution in the presence of triethylamine and copper sulfate in acetonitrile medium to afford the acid **375**. The *N*-Boc-protected amino acid was transformed into the azide moiety **376** in three consecutive steps and subsequent Boc-deprotection followed by coupling with **375** under standard conditions afforded the macrocyclic precursor **377**. Intramolecular cycloaddition with CuI/DBU catalytic mixture in dichloromethane at room temperature for 12 h afforded macrocycle **378** in 48% yield. Finally, after two consecutive steps, the desired triazole-based macrocycle **390** was achieved (Scheme 44). After investigating the biological properties of **379–390**, it was reported that these macrocycles showed inhibition against novovirus 3C-Like protease.

In 2019, the Groutas group extended their previous synthetic work⁹ and established a few macrocyclic inhibitors of novovirus 3CLpro, **391–393**, utilizing similar multistep synthesis and click-methodology as described earlier (Figure 4).⁴³ The FRET NV 3CL protease assay along with the examination of the effects of macrocycles on virus replication against NV or MNV gave results that were comparable to those of a few previously synthesized macrocycles.⁹

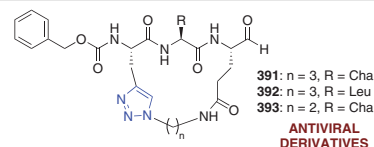
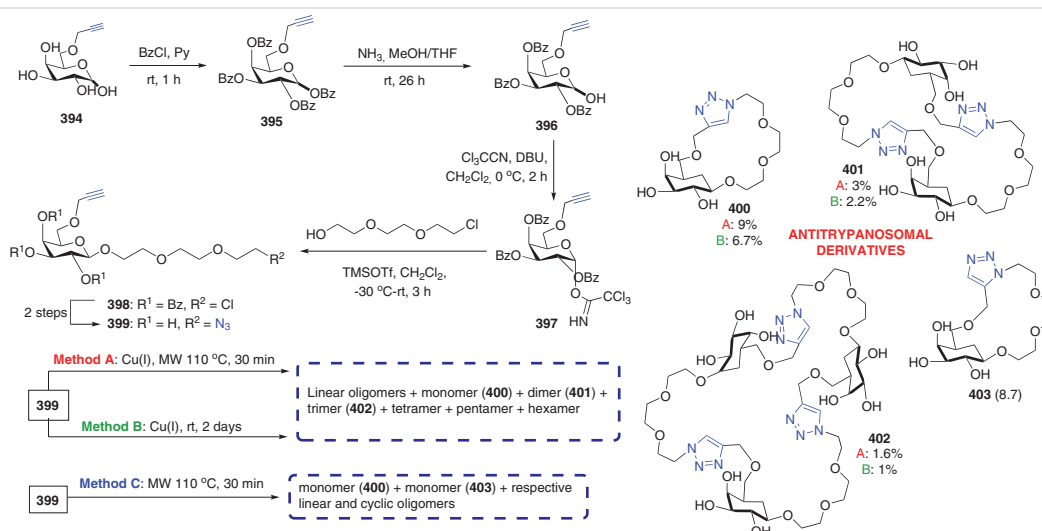


Figure 4 Antiviral agents **391–393**

8 Anti-trypanosomal Derivatives

American trypanosomiasis, also known as Chagas disease, is a life-threatening condition caused by the parasite *Trypanosoma cruzi* transmitted through the faeces of triatomine bugs. Millions of people, especially in regions like Latin America, are affected every year with this fatal disease, and there is a desperate need for treatment.

Campo *et al.*, in 2015, showed their interest in developing triazole-linked macrocyclic inhibitors of *T. cruzi* transsialidase (TcTS), which was found to be a potential drug target for the aforementioned disease (Scheme 45).⁴⁴ In order to achieve the galactose monomer **399**, *O*-propargyl-D-galactopyranose **394**, was chosen as the starting material. With suitable benzoylation of **394** followed by exposure to ammonia in methanolic-THF medium, the hemiacetal **396** was synthesized. With further treatment with trichloroacetonitrile and DBU, compound **397** was formed and subsequently activated with trimethylsilyl trifluoromethanesulfonate and 2-(2-(2-chloroethoxy)ethoxy)ethanol to give the β -glycoside **398**. Through two sequential reactions, the chlorinated fragment **398** was converted into the azide **399** and then tested under two different CuAAC reaction conditions. The first method (A) involved subjecting **399** to Cu-



Scheme 45 Synthesis of macrocycles **400–403** with anti-trypanosomal activity

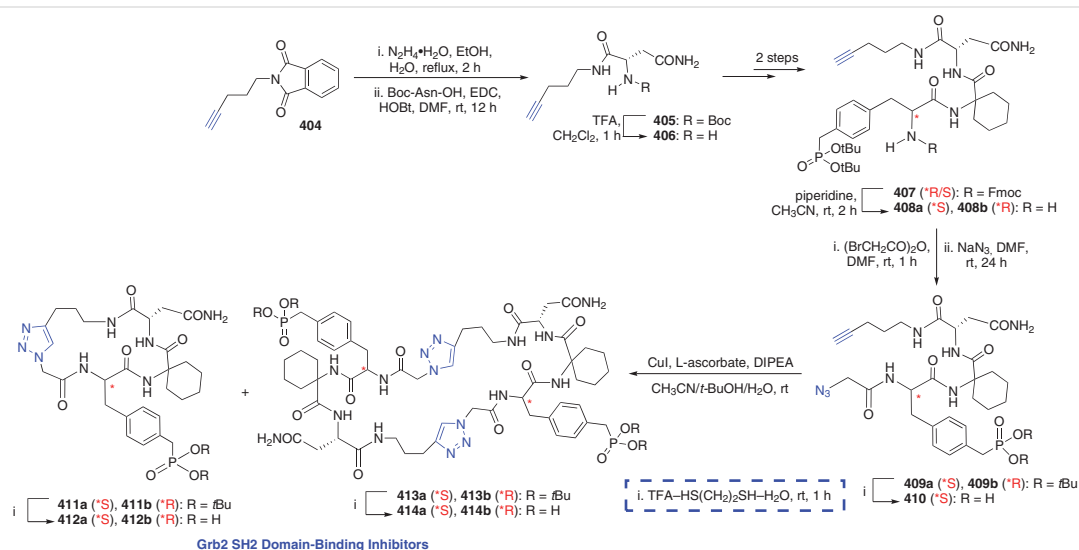
SO₄/Cu turnings in DMF under microwave irradiation at 110 °C for 30 min, whereas the second reaction (B) was conducted at ambient temperature and continued for 2 days; both the reactions afforded linear as well as cyclic products. The cyclic oligomers of various ring sizes (monomer **400**, dimer **401**, trimer **402** and so on) were obtained by utilizing the 1,4-disubstituted triazole as connectors. When the component **399** was separately exposed to uncatalyzed microwave conditions for 30 min (Method C), the 1,4-disubstituted triazole based macrocycle **400** and the 1,5-disubstituted triazole based macrocycle **403** were obtained as products, along with their respective linear oligomers. Through biological investigation, it was reported that the macrocycles serve as acceptor substrates for the enzyme *trans*-sialidase related with host cell invasion by *T. cruzi* and were also noted to inhibit the invasion of *T. cruzi* into bovine macrophages.

9 Derivatives with Miscellaneous Activities

The growth factor receptor-bound protein 2 (Grb2) is a favourable drug target for researchers, being a SH2 domain-containing signal transducer. In 2006, Choi *et al.* synthesized a series of SH2 domain-binding inhibitors **411–414a,b** via CuAAC reaction (Scheme 46).⁴⁵ The synthetic procedure commenced with the preparation of key fragment **409a,b** using the alkyne moiety **404** as the starting material. After heating at reflux in ethanol with hydrazine, the amine thus produced was further coupled with *N*-Boc L-Asn using HOBt and EDC to afford the Boc-protected amide **405**. TFA-mediated deprotection of **405** formed **406**, which was then subjected to two subsequent steps to synthesize the tripeptide **407**. On attaining this compound in the form of an in-

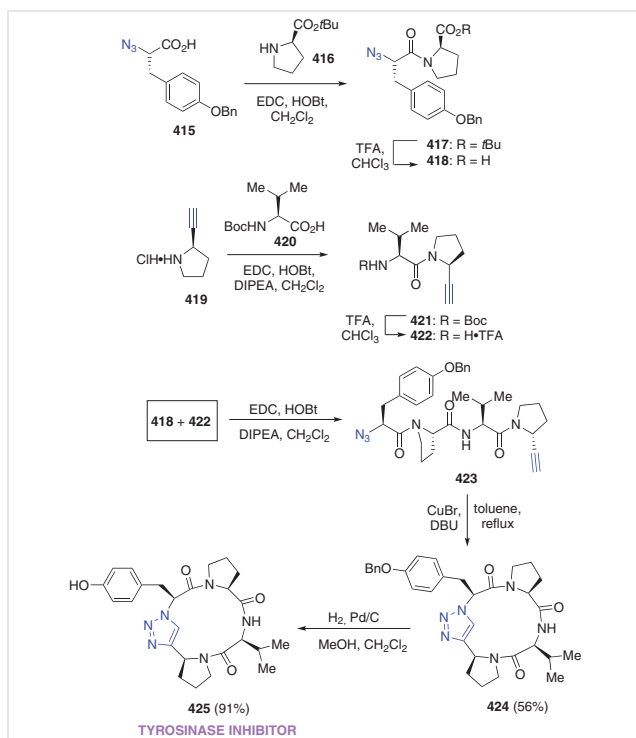
separable epimeric mixture, further *N*-Fmoc removal resulted in separation of the amines and production of the diastereomers **408a** and **408b**. The macrocyclic precursors **409a,b** were prepared by treating **408a,b** with bromoacetic anhydride and subsequent addition of sodium azide. Removal of the *t*-Bu group and exposure to copper sulfate, L-ascorbate and DIPEA in acetonitrile-*t*-BuOH/H₂O solvent system at room temperature then afforded the monomeric macrocycles **411a,b** along with the dimers **413a,b**. The cycloaddition reaction produced the monomers as a majority at 1 μM substrate concentration, whereas the dimers were obtained predominantly at 2 μM substrate concentration. Finally, cleavage of the *t*-butyl esters produced the target monomeric (**412a,b**) and dimeric (**414a,b**) macrocycles. Surface plasmon resonance (SPR) was used to evaluate the Grb2 SH2 domain-binding affinities of the newly synthesized macrocycles. It was found that the (*R*)-isomeric-macrocycles **412b** and **414b** displayed binding constants above 1 μM. The monomeric (*S*)-macrocycle **412a** bound with sub-micromolar affinity whereas its corresponding dimer **414a** exhibited more than 50-fold higher binding affinity.

A potent tyrosinase inhibitor *cyclo*-[Pro-Tyr-Pro-Val] (**432**), was isolated from the 'good bacteria' *L. helveticus*. Being interested in developing synthetic analogues of the natural cyclotetrapeptide, in 2007, the van Maarseveen group achieved two triazole analogues (**425**, **431**) of the aforementioned compound (Scheme 47 and Scheme 48).¹¹ The process began with the preparation of the linear precursor **423** through an initial coupling of the acid **415** and protected proline **416** to develop the azido-amide **417**. Further deprotection of **417** led to the synthesis of a key fragment **418** (Scheme 47). A similar EDC-HOBt-mediated coupling between alkyne **419** and protected valine **420** afforded **421**, which, upon Boc deprotection, afforded the second key



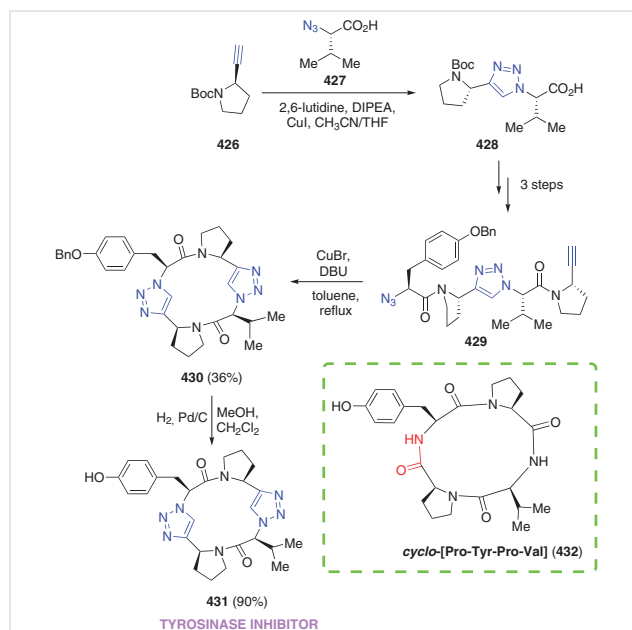
Scheme 46 Synthesis of SH2 domain-binding inhibitors **411–414a,b**

fragment **422**. Subsequently, the macrocyclic precursor **423** was synthesized through peptide coupling of **418** and **422** in the presence of EDC, HOBT, DIPEA in dichloromethane and finally subjected to macrocyclization through CuBr-mediated CuAAC reaction with DBU in refluxing toluene to furnish the triazole-fused macrocycle **424** in 56% yield. Pd-catalyzed hydrogenation of **424** finally afforded the desired analogue **425** in 91% yield (Scheme 48). In order to prepare the other triazole analogue **431**, the alkyne moiety **426** was initially coupled with the azide moiety **427** to graft the triazole based key fragment **428**. Compound **428** was further exposed to three consecutive reactions to obtain the linear macrocyclic precursor **429**. A similar CuAAC methodology was applied to **429**, which furnished the cyclotetrapeptide **430** in 36% yield. Benzyl group deprotection of **430** finally helped in grafting the desired analogue **431** in 90% yield (Scheme 48). Biological investigation of the synthesized macrocycles **425** and **431** was carried out by comparison of their inhibitory activity with their parent compound **432**. It was reported that the analogues exhibited three-fold increase in inhibition against mushroom tyrosinase.



Scheme 47 Synthesis of tyrosinase inhibitor

In 2011, Ingale and Dawson described the synthesis of structurally constrained peptides through side-chain macrocyclization following CuAAC reaction (Scheme 49).⁴⁶ Commercially available Tenta-gel resin was treated through Fmoc SPPS protocol to produce the protected resin-bound peptide **433**. The key macrocyclization was conducted with CuBr, sodium ascorbate, 2,6-lutidine and DIPEA in DMSO for



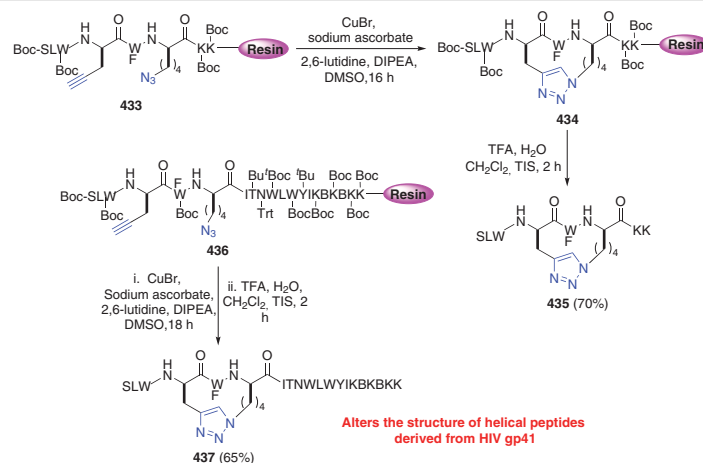
Scheme 48 Synthesis of tyrosinase inhibitor

16–18 h at room temperature to afford the triazole-based intermediate **434**. Subsequent removal of protecting groups and resin cleavage provided the cyclized product **435** in 70% yield. In order to show the usefulness of this reaction in complex systems, full-length MPER epitope of gp41 668–683 was produced. The resin bound peptide **436** was exposed to similar macrocyclization conditions as stated earlier followed by deprotection and resin cleavage to afford the triazole-fused product **437** in 65% yield. Upon evaluating the binding of the triazole-constrained peptides to 4E10 and Z13e1, they were noted to alter the structure of helical peptides obtained from HIV gp41.

Sunflower trypsin inhibitor-1 (SFTI-1) is a cyclic peptide framework favoured by researchers synthesizing peptide-based pharmaceuticals as it acts a potent inhibitor of trypsin. With a wide range of applications in drug design, SFTI-1 is particularly targeted to serine proteases and GPCRs. The Kolmar group, in 2011, developed three triazole-based derivatives (**440**, **441** and **444**) of a peptide variant of SFTI-1 (**445**; Figure 5) by utilizing both CuAAC and RuAAC methodologies (Scheme 50).⁴⁷ Commercially available SPPS building blocks Fmoc-L-propargylglycine (Fmoc-Pra-OH) and Fmoc-L-azidoalanine (Fmoc-Aza-OH) or Fmoc-L-azido-



Figure 5 A peptide variant of SFTI-1

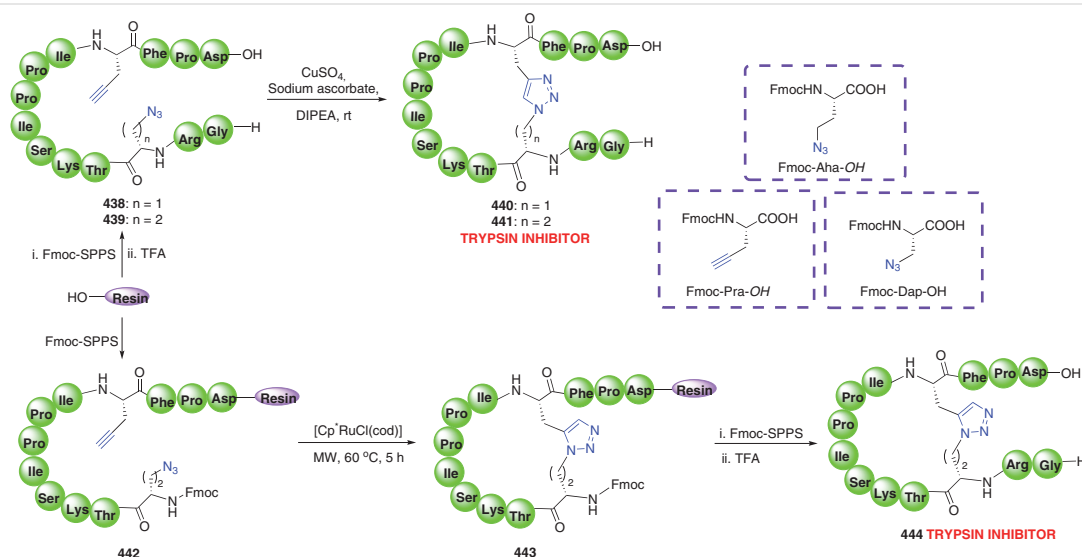


Scheme 49 Synthesis of peptide macrocycle **437**

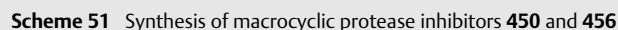
homoalanine (Fmoc-Aha-OH) were utilized to afford the macrocyclic precursors **438** and **439**, respectively. Subsequent TFA-mediated cleavage with further macrocyclization undertaken in presence of copper sulfate, sodium ascorbate and DIPEA at room temperature resulted in the formation of the 1,4-disubstituted triazole-linked peptides **440** and **441**, respectively. Application of RuAAC methodology to the unprotected peptide **439** led to a mixture of undesired products, thus prompting the researchers to develop a different linear precursor **442**. The protected peptide **442** was subjected to [Cp^{*}RuCl(cod)] catalyzed reaction under microwave irradiation at 60 °C for 5 h and the 1,5-disubstituted triazole-linked macrocycle **443** was obtained. The desired macrocycle **444** was obtained after the introduction of SPPS building block and consecutive acidic cleavage. Kinetic studies using active-site titrated trypsin made

it clear that different modes of macrocyclization affected the inhibitory activity of the peptides significantly. The 1,5-disubstituted triazole-based macrocycle **444** was reported to retain inhibition in a range comparable to its parent peptide **445** (Figure 5), whereas the 1,4-disubstituted triazole-based macrocycles **440** and **441** showed a decline in inhibition.

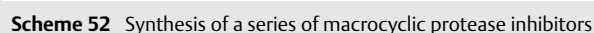
In 2013, Peheré *et al.* designed triazole-fused macrocyclic protease inhibitors (Scheme 51 and Scheme 52).⁴⁸ For the preparation of the macrocycle **450**, initial coupling in between the dipeptide **446** with the azide moiety **447** under standard EDCI-HOBt conditions gave rise to the tripeptide **448**, which further underwent macrocyclization in the presence of CuBr and DBU in dichloromethane for 7 h at room temperature to afford the macrocycle **449** (71%). Subsequently, **449** was reduced with lithium borohydride and



Scheme 50 Synthesis of trypsin inhibitors **440**, **441** and **444**



In a similar manner, the alkyne fragment **457** was coupled with **452** under AAC reaction conditions using copper sulfate and sodium ascorbate to furnish the triazole-linked moiety **458** (63%). Further Boc deprotection followed by



HATU/HOAt mediated amide formation resulted in the development of the triazole-fused macrocycle **460** in 48% yield (Scheme 52). Two subsequent steps finally afforded the desired compound **461** in 80% yield. The macrocyclic precursor **462**, constituting both the azide and alkyne parts, underwent intramolecular CuAAC reaction with CuBr under the aforementioned conditions to give **463** (70%), which, upon further oxidation with DMP, afforded macrocycle **465** in 73% yield. To the authors amazement, when compound **462** was left at room temperature for a few months, the 1,5-disubstituted triazole **464** (65%) was received. Upon further oxidation, the macrocycle **466** was obtained in 71% yield. Biological evaluation of the macrocycles showed all compounds displayed inhibition towards Cathepsin S (Cat S), a protease related to tumour growth, autoimmune diseases, and osteoporosis etc. Compound **466** was found to be on par with **465** when tested for inhibition towards the proteases calpain II (implicated in stroke, cataracts etc.), Cat S, and Chymotrypsin-like (CT-L) (anticancer therapeutic target). It was also found to exhibit a fourfold decrease in potency for Cathepsin L in comparison with **465**.

After isolation in 2010, the natural product Palmyrolide A had been identified as having neuroprotective activity as it suppressed neuronal spontaneous calcium ion oscillations through its voltage-gated sodium channel (VGSC) blocking ability. Thus, researchers have always considered Palmyrolide A to be a favourable target in CNS drug discovery. In 2016, Philkhana *et al.* synthesized two triazole based analogues (**471**, **472**) of Palmyrolide A and investigated their bioactivities (Scheme 53).¹² The process began by subjecting compound **467** to ozonolysis with subsequent Seyferth–Gilbert homologation using the Ohira Bestmann reagent to afford the alkyne **468**. TCBC-mediated esterification of **468** with 6-azidohexanoic acid **469** produced the macrocyclic precursor **470**, which was finally clicked intramolecularly with CuI in MeOH/PEG400 (1:2) medium at 80 °C under sealed conditions. The desired triazole-fused macrocycles **472** and **471** were obtained in a combined yield of

66% in a 2:1 ratio. Biological evaluation of the macrocycles was conducted to check their interaction with VGSC. Their inhibitory activity against the veratridine-stimulated Na⁺ influx in murine primary neuronal cultures proved that the triazole-containing moieties did not show much potency; instead, **472** exhibited a fivefold decrease in activity compared with its parent compound Palmyrolide A (Figure 6).

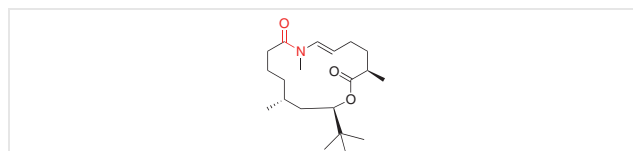
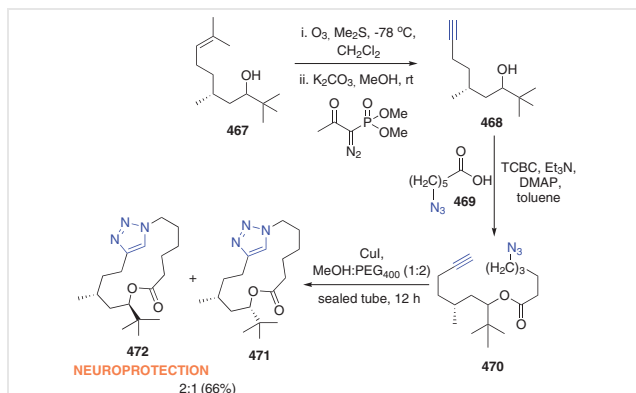


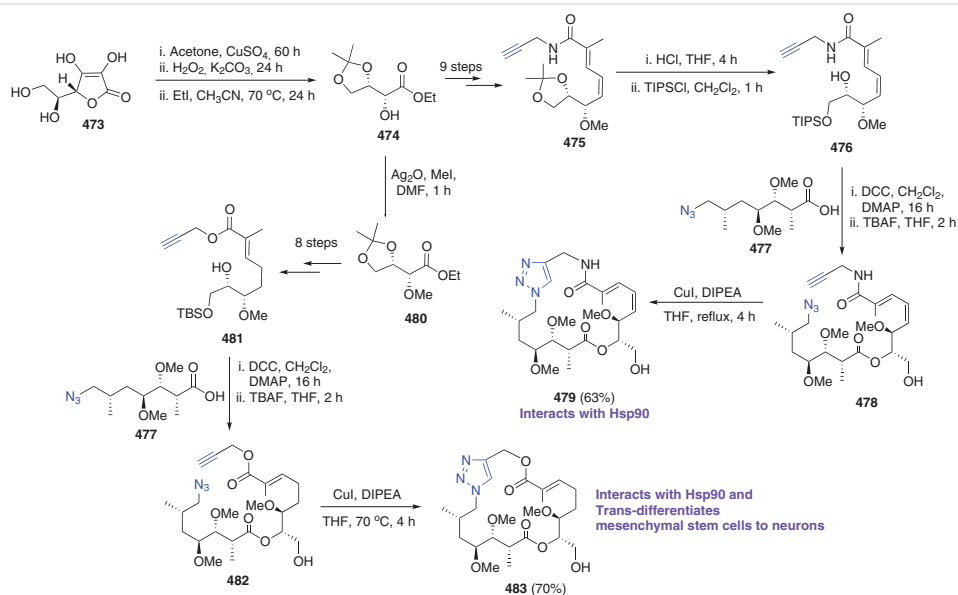
Figure 6 (–)-Palmyrolide A

Jogula *et al.*, in 2017, synthesized some ‘Geldanamycin’ inspired triazole-based macrocycles by employing CuAAC reaction as the crucial macrocyclization step and evaluated their bioactivities (Scheme 54).⁴⁹ The preparation of the target molecules was initiated from L-ascorbic acid (**473**) as it was converted into ester fragment **474** following a reported method. Several consecutive steps afforded the fragment **475**, which was subsequently acidified to cleave the dioxolane moiety and treated with triisopropylsilyl chloride to achieve **476**. The macrocyclic precursor **478** was next achieved through DCC/DMAP coupling of the separately synthesized azido-acid **477** and the alcohol **476**. The final macrocyclization occurred via intramolecular cycloaddition reaction by utilizing CuI/DIPEA catalytic system in refluxing THF, and resulted in the desired product **479** in 63% yield. By following a similar methodology, ester **480** was converted into the TBS-protected alkyne fragment **481**, which was further coupled with **477** to produce the macrocyclic precursor **482**. This moiety was intramolecularly clicked using the aforementioned catalyst at 70 °C to graft the macrocycle **483** (70%). In order to assess these novel macrocycles biologically, initial molecular docking simulations of **479** and **483** were investigated with Hsp90. It was reported that **483** exhibited better binding with the ATP binding site of Hsp90 protein than geldanamycin. The synthesized macrocycles exhibited the ability to trans-differentiate human umbilical cord tissue-derived mesenchymal stem cells to neurons. By monitoring the phenotypic changes occurring within the cells, some selected biomarkers viz. nestin, agrin and RTN4 were identified to be present in the transformed neuronal cells with **483**.

The melanocortin system is known to be involved in the regulation of physiological functions like feeding behaviour, inflammation, pigmentation, exocrine gland function and more. In 2018, Tala *et al.* reported the synthesis of some triazole-bridged peptidomimetics and evaluated them as mouse melanocortin receptors (Scheme 55 and Scheme 56).⁵⁰ Initially, the linear peptide **484** was synthesized by following the Fmoc/*t*-Bu SPPS method on Rink-amide MBHA resin. The solid-phase assembly in furnishing **484**



Scheme 53 Synthesis of Palmyrolide-A analogue **472**

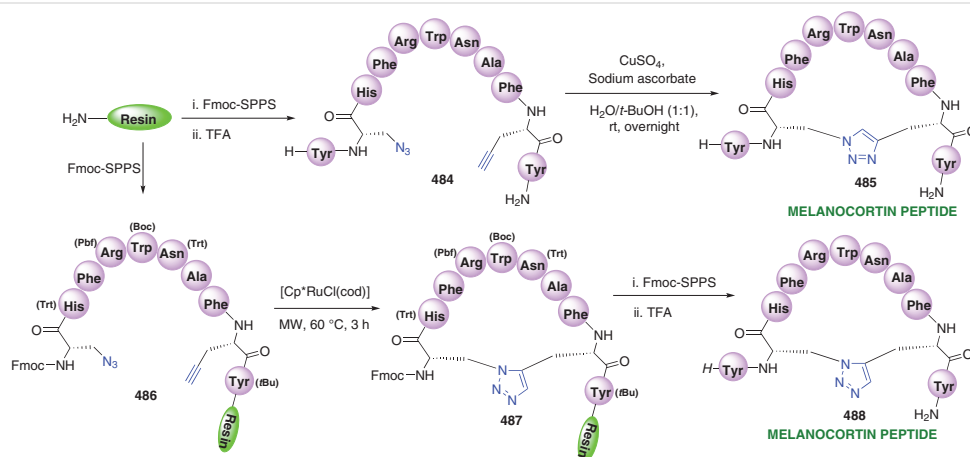


Scheme 54 Synthesis of Geldanamycin inspired macrocycles **479**, **483**

had introduced both the alkyne and azide groups within the system by replacing the N^{α} -Fmoc-Cys-OH residues with N^{α} -Fmoc-L-Pra-OH and N^{α} -Fmoc-L-Aza-OH amino acids within the peptide template **494** (Figure 7). The macrocyclic precursor **484** favourably underwent intramolecular CuAAC reaction conducted overnight using copper sulfate-sodium ascorbate in $H_2O/tBuOH$ solvent system at room temperature and afforded the desired 1,4-disubstituted triazole-fused macrocyclic peptide **485** (Scheme 55). In a similar manner, the linear peptide **486** was also prepared by coupling the amino acids on resin using the aforementioned strategy. Subsequently, macrocyclization was conducted with catalytic $[Cp^*RuCl(cod)]$ under microwave (30 W) at 60 °C for 3 h to graft the compound **487** on resin. After sub-

jecting to further coupling of Tyr and subsequent TFA-mediated cleavage, the 1,5-substituted triazole-fused macrocyclic peptide **488** was obtained.

The effects of ring size on macrocyclization were further investigated by the team and, henceforth, the N^{α} -Fmoc-L-Aza-OH residues in **494** were replaced with N^{α} -FmocL-Orn(N_3)-OH amino acids to develop the linear peptide **489** through the Fmoc/tBu SPPS method. Subsequently, **489** was coupled with 1,3-diethynylbenzene **490** by following the intermolecular copper sulfate-sodium ascorbate catalyzed reaction in the presence of tris(3-hydroxypropyl-triazolylmethyl)amine in a similar manner to that described earlier. This yielded the target macrocyclic 1,4-disubstituted bis-triazole-fused peptide **491** predominantly (Scheme



Scheme 55 Synthesis of macrocyclic peptides **485**, **488**

56). The peptide resin **492**, afforded in a way same as the linear precursors, was coupled with **490** through intermolecular RuAAC reaction using $[\text{Cp}^*\text{RuCl}(\text{cod})]$ under microwave conditions as stated earlier. Through subsequent deprotection, resin-cleavage and purification, the 1,5-disubstituted bis-triazole-macrocytic peptide **493** was obtained as the major product. With the generated macrocycles in hand, the pharmacological assessment with mouse melanocortin receptors mMC1R, mMC3R, mMC4R, and mMC5R was conducted. Their ability to stimulate intracellular cAMP signalling was tested in HEK293 cells. The macrocyclic peptide **485** showed 41-, 13-, 14-, and 7-fold decrease in potency at the mMC1R, mMC3R, mMC4R, and mMC5R, respectively, in comparison to the template peptide **494**. The peptide **488** was noted to exhibit an increase in potency at the mMC3R and mMC5R, while maintaining potent nanomolar agonist activity with mMC1R and mMC4R in contrast with the potency of **488**. Compound **488** was also found to show a fivefold decrease in potency at mMC4R in comparison with **494** and a 29-fold reduced potency at mMC1R. Peptides **491** and **493** were seen to display modest selectivity for mMC5R.

White *et al.*, in 2020, established a series of triazole-linked cyclic peptides using the SFTI-1 framework and assayed them against serine protease inhibitors (Scheme 57).⁵¹ Commercially available β -azidoalanine (Aza) or γ -azidohomoalanine (hAza) and propargylglycine (Prg) were assembled by Fmoc SPPS on 2-chlorotrityl chloride resin **495**. Subsequent resin cleavage and backbone cyclization

brought the azide and alkyne groups close to each other. Further TFA-cleavage was followed by CuAAC reaction with copper sulfate, THPTA and sodium ascorbate at 37 °C for 3 h resulted in the formation of 1,4-disubstituted triazole-linked peptide macrocycles **500d–f** and **501d–f**. On exposing the protected peptide to RuAAC reaction with $[\text{Cp}^*\text{RuCl}(\text{cod})]$ catalyst in DMF at 80 °C for 18 h, the 1,5-disubstituted triazole-linked peptide was obtained. Final deprotection led to the production of the target compounds **500b,c**, **502b**, **501b,c** and **503b**. The inhibitory activities of triazoles **500b–f** were evaluated against trypsin using SFTI-1 as a reference. Compounds **500b,c** were found to be more potent compared with the others, whereas **500b** was reported to retain maximum inhibition when compared with SFTI-1. The other triazole-based peptide analogues **502b**, **501b** and **503b** were screened for inhibition against kallikrein-related peptidase 7 (KLK7), plasmin and matriptase. Compound **502b** exhibited a sevenfold lower inhibitory activity than its parent **502a** when assayed upon KLK7 protease involved in skin disorders. Compound **501b** showed 62-fold less inhibition compared with **501a** after being evaluated against plasmin, a protease related to fibrinolysis. Furthermore, the analogues **501c–f** exhibited extreme loss in potency (>6300-fold) when assayed against the same, confirming that **501b** remained the most favourable disulfide mimetic. The other analogue **503b** was noted to display 120-fold less inhibition than **503a** after being screened against matriptase, a membrane-anchored protease involved in epithelial tumours. The triazole-linked peptides **500b–503b** were tested against human serum and were found to resist degradation. On being investigated against liver S9 assays, **500b–503b** were reported to be stable with half-lives greater than 200 min.

Kulsi *et al.*, in 2020, designed an amide-based triazole-linked macrocycle **511** through cyclo-oligomerization (Scheme 58).⁵² The synthetic route progressed with the

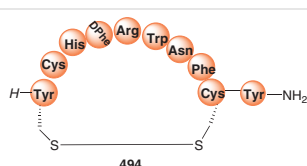
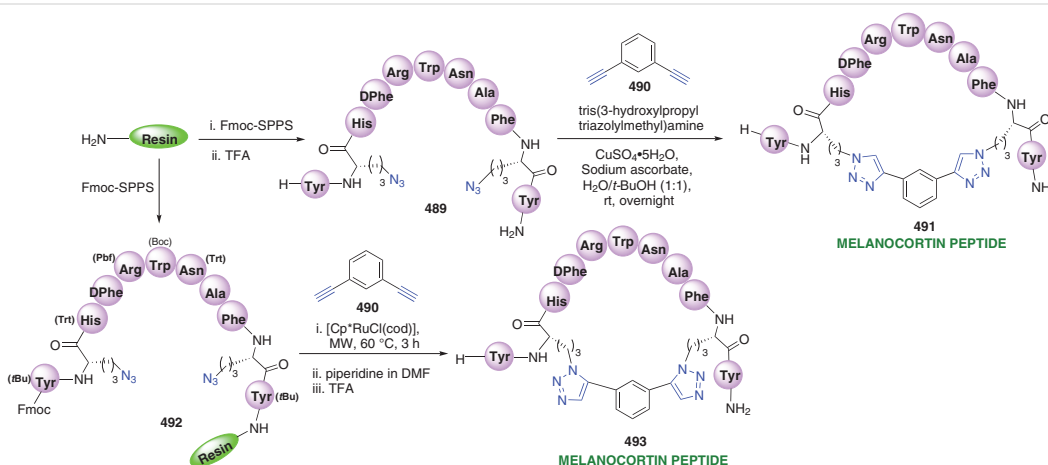
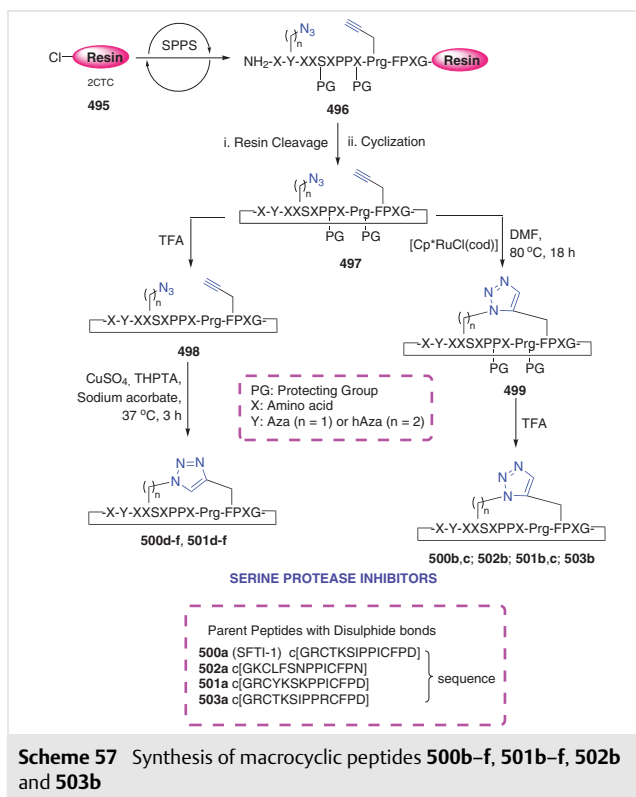


Figure 7 A peptide template



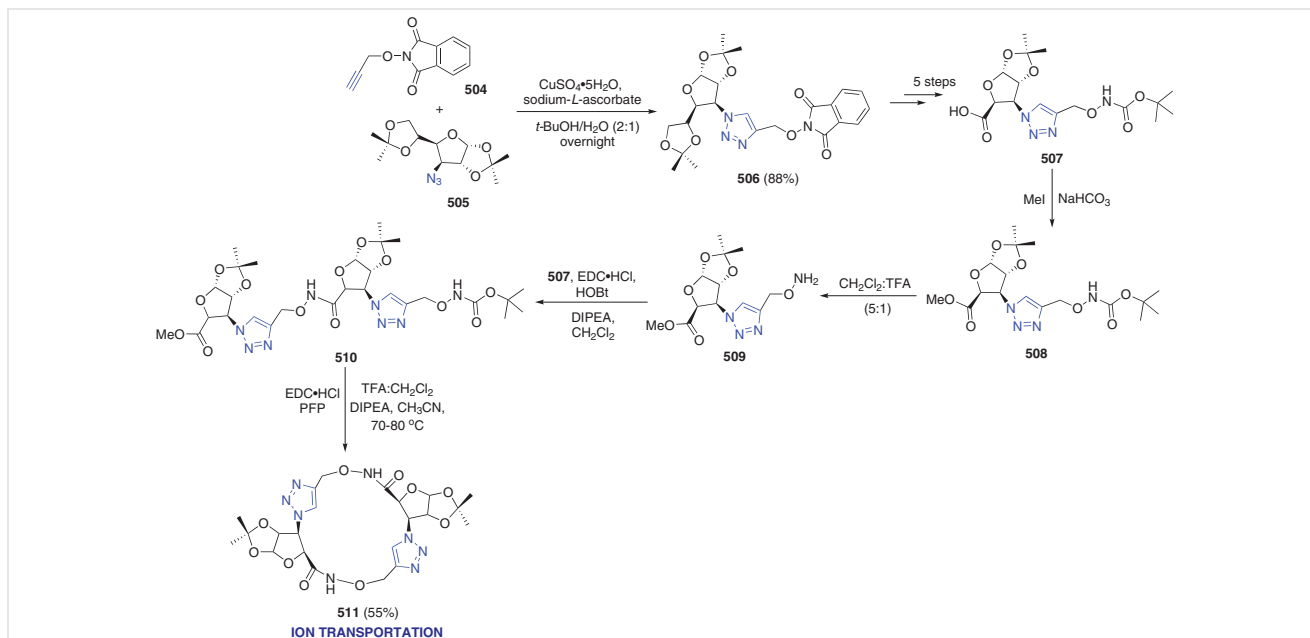
Scheme 56 Synthesis of macrocyclic peptides **491**, **493**



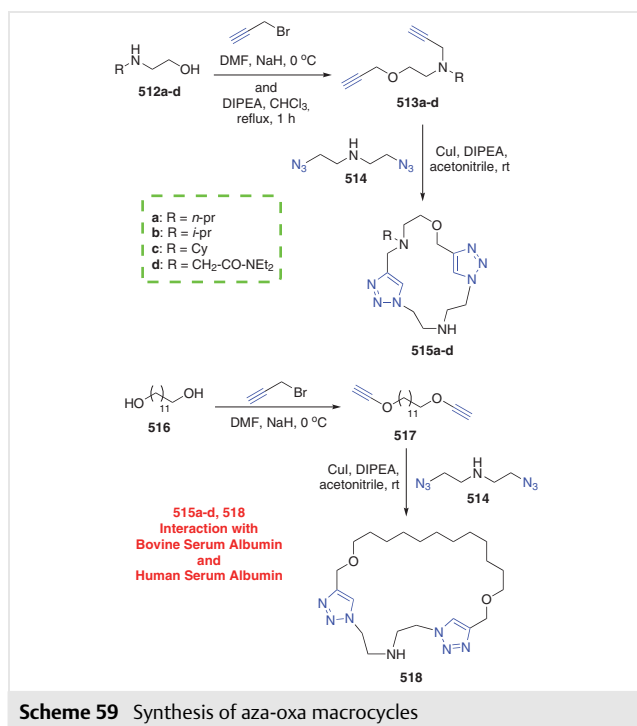
azide-alkyne cycloaddition between *O*-phthalimide-protected propargyl alcohol **504** and azido-glucose **505** using copper sulfate and sodium ascorbate in *t*-BuOH/ H_2O medium to afford the triazole **506** in 88% yield. Five consecutive

steps led to the production of the intermediate **507**, which was further subjected to sequential protection-deprotection to furnish **509**. Subsequently, the fragments **507** and **509** were coupled together to form amide **510** under EDC/HOBt conditions. The final macrocyclization to yield the cyclic peptide **511** (55%) took place via hydrolysis and activation with penta-fluorophenyl ester (PFP) with gradual peptide coupling. Through several assessments, macrocycle **511** was found to be an electroneutral and anion receptor. With an incredible ability to distinguish in between ions, the macrocycle exhibited a preference towards Cl^- ion and served as a scaffold for ion transportation, thus imposing cancer cell death by disruption of ionic homeostasis.

In 2022, Cheekatla *et al.* developed a aza-oxa based macrocycles by employing CuAAC reaction and evaluated their biological properties (Scheme 59).⁵³ The synthetic procedure commenced by subjecting the amine-hydroxyl derivatives **512a-d** to *O*-propargylation with propargyl bromide by using NaH in DMF at 0 °C and subsequent *N*-propargylation in the presence of DIPEA in refluxing chloroform to afford the alkyne moieties **513a-d**. These alkynes underwent intermolecular CuAAC reaction with bis(2-azidoethyl)amine **514** using catalytic CuI and DIPEA in acetonitrile medium at room temperature for 12–24 h to afford the triazole-fused macrocycles **515a-d**. For the other macrocycle **518**, diol **516** was initially converted into its corresponding di-propargylated moiety **517** by the action of propargyl bromide and NaH in DMF at 0 °C and was further treated under similar click-conditions as described earlier. By studying the fluorescence properties for the interaction between the macrocycles with bovine serum albumin (BSA)

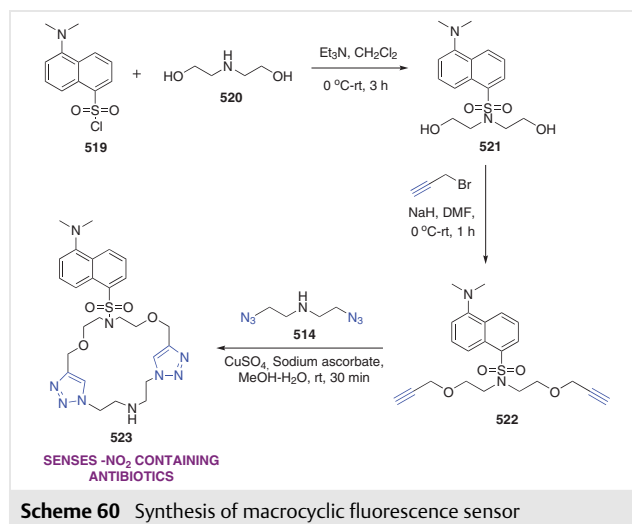


and human serum albumin (HSA), it was reported that all the compounds exhibited a varied range of interactions. The macrocycles that interacted well with the proteins showed fluorescence quenching. Upon calculating the binding constants for the interaction of macrocycles and BSA, **518** was noted to have the highest binding while the other macrocycles **515a–d** exhibited moderate binding. Furthermore, the fluorescence studies of **518** with HSA showed that it had the highest interaction and quenching while the other macrocycles displayed moderate results.



Scheme 59 Synthesis of aza-oxa macrocycles

Thurakkal *et al.* synthesized a triazole-based macrocyclic fluorescence sensor in 2023 for the detection of antibiotics containing nitro groups (Scheme 60).⁵⁴ The envisioned procedure commenced with the reaction of dansyl chloride **519** with diethanolamine **520** in the presence of triethylamine to afford **521**. After subsequent exposure to propargyl bromide, **521** was converted into the dialkyne-moiety **522**. The final macrocyclization was conducted in the presence of the azide moiety **514** through CuAAC reaction with copper sulfate and sodium ascorbate in MeOH/H₂O medium at room temperature for 30 min to furnish the macrocycle **523**. The photophysical studies of **523** along with its interaction with several antibiotic drugs such as dimetridazole (DMI), nitrofurantoin (NFT), and nitrofurazone (NFZ) were conducted. Fluorescence spectroscopy and molecular docking showed that DTMC sensed the nitro-containing compounds and also showed favourable interaction with proteins.



Scheme 60 Synthesis of macrocyclic fluorescence sensor

10 Conclusion

We have reported several synthetic methodologies for the preparation of biologically active 1,2,3-triazole-fused macrocyclic compounds having ring sizes of 12 to 60 members. Many of them have been constructed through peptide linkages. In most of the cases, the renowned Cu-catalyzed azide-alkyne cycloaddition reaction led to the 1,4-disubstituted 1,2,3-triazoles, whereas the 1,5-disubstituted 1,2,3-triazole-fused macrocycles were obtained *via* Ru-catalyzed cycloaddition. The thorough literature survey demonstrates that the azide-alkyne cycloaddition is a versatile method that does not require drastic reaction conditions. It was observed that even when further functionalization of the triazole-linked scaffolds was conducted, in order to obtain the target bioactive compounds, the triazole moieties remained unaffected. Researchers also synthesized analogues of a few naturally occurring bioactive macrocycles involving azide-alkyne cycloaddition strategies.^{4,17,21,24} The macrocycles described herein hold promising biological properties *viz.* anticancer, antibacterial, antiviral, anti-trypanosomal, antilarval, anti-inflammatory etc. The bioactivities of these triazole-based analogues were retained, which showed the nitrogen-rich triazole moiety to be an extremely useful moiety in drug discovery. We anticipate that this review article will pique the curiosity of various researchers in establishing several methodologies to graft biologically relevant triazole-fused macrocycles.

Conflict of Interest

The authors declare no conflict of interest.

Funding Information

We sincerely thank the Department of Science and Technology and Biotechnology (Government of West Bengal) for providing financial assistance until the year 2022. N. Jahan is grateful to the Government of West Bengal for her research fellowship, Swami Vivekananda Merit Cum Means Fellowship.

Acknowledgment

The authors acknowledge the Department of Science and Technology, Ministry of Science and Technology (New Delhi) for providing the HRMS instrument (Thermo Scientific) under the FIST programme.

References

- (1) Liang, Y.; Fang, R.; Rao, Q. *Molecules* **2022**, *27*, 2837.
- (2) (a) Marsault, E.; Peterson, M. L. *J. Med. Chem.* **2011**, *54*, 1961. (b) Cheekatla, S. R.; Barik, D.; Anand, G.; Mol, K. M. R.; Porel, M. *Organics* **2023**, *4*, 333. (c) Medved'ko, A. V.; Gaisen, S. V.; Kalinin, M. A.; Vatsadze, S. Z. *Organics* **2023**, *4*, 417. (d) Begnini, F.; Poongavanam, V.; Over, B.; Castaldo, M.; Geschwindner, S.; Johansson, P.; Tyagi, M.; Tyrchan, C.; Wissler, L.; Sjö, P.; Schiesser, S.; Kihlberg, J. *J. Med. Chem.* **2021**, *64*, 1054.
- (3) Jahan, N.; Ansary, I. *SynOpen* **2023**, *7*, 209.
- (4) Horne, W. S.; Olsen, C. A.; Beierle, J. M.; Montero, A.; Ghadiri, M. R. *Angew. Chem. Int. Ed.* **2009**, *48*, 4718.
- (5) Day, J. E. H.; Sharp, S. Y.; Rowlands, M. G.; Aherne, W.; Workman, P.; Moody, C. J. *Chem. Eur. J.* **2010**, *16*, 2758.
- (6) Duan, X.; Zhang, Y.; Ding, Y.; Lin, J.; Kong, X.; Zhang, Q.; Dong, C.; Luo, G.; Chen, Y. *Eur. J. Org. Chem.* **2012**, 500.
- (7) Prabhakaran, P.; Subaraja, M.; Rajakumar, P. *ChemistrySelect* **2018**, *3*, 4687.
- (8) Anandhan, R.; Kannan, A.; Rajakumar, P. *Synth. Commun.* **2017**, *47*, 671.
- (9) Mandadapu, S. R.; Weerawarna, P. M.; Prior, A. M.; Uy, R. A. Z.; Aravapalli, S.; Alliston, K. R.; Lushington, G. H.; Kim, Y.; Hua, D. H.; Chang, K.; Groutas, W. C. *Bioorg. Med. Chem. Lett.* **2013**, *23*, 3709.
- (10) Rana, R.; Dolma, S. K.; Maurya, S. K.; Reddy, S. G. E. *Toxin Rev.* **2020**, *39*, 197.
- (11) Bock, V. D.; Speijer, D.; Hiemstra, H.; van Maarseveen, J. H. *Org. Biomol. Chem.* **2007**, *5*, 971.
- (12) Philkhana, S. C.; Mehrotra, S.; Murray, T. F.; Reddy, D. S. *Org. Biomol. Chem.* **2016**, *14*, 8457.
- (13) (a) Ansary, I.; Roy, H.; Das, A.; Mitra, D.; Bandyopadhyay, A. K. *ChemistrySelect* **2019**, *4*, 3486. (b) Silvestri, I. P.; Andemarian, F.; Khairallah, G. N.; Yap, S. W.; Quach, T.; Tsegay, S.; Williams, C. M.; O'Hair, R. A. R.; Donnelly, P. S.; Williams, S. J. *Org. Biomol. Chem.* **2011**, *9*, 6082. (c) Johansson, J. R.; Beke-Somfai, T.; Stålsmeden, A. S.; Kann, N. *Chem. Rev.* **2016**, *116*, 14726. (d) Roshandel, S.; Suri, S. C.; Marcischak, J. C.; Rasul, G.; Surya Prakash, G. K. *Green Chem.* **2018**, *20*, 3700. (e) Dar, B. A.; Bhowmik, A.; Sharma, A.; Sharma, P. R.; Lazar, A.; Singh, A. P.; Sharma, M.; Singh, B. *Appl. Clay Sci.* **2013**, *80–81*, 351.
- (14) Jahan, N.; Das, A.; Ansary, I. *ChemistrySelect* **2022**, *7*, e202201831.
- (15) Chen, J.; Nikolovska-Coleska, Z.; Yang, C.; Gomez, C.; Gao, W.; Krajewski, K.; Jiang, S.; Roller, P.; Wang, S. *Bioorg. Med. Chem. Lett.* **2007**, *17*, 3939.
- (16) Singh, E. K.; Nazarova, L. A.; Lapera, S. A.; Alexander, L. D.; McAlpine, S. R. *Tetrahedron Lett.* **2010**, *51*, 4357.
- (17) Nahrwold, M.; Bogner, T.; Eissler, S.; Verma, S.; Sewald, N. *Org. Lett.* **2010**, *12*, 1064.
- (18) Piralì, T.; Faccio, V.; Mossetti, R.; Grolla, A. A.; Micco, S. D.; Bifulco, G.; Genazzani, A. A.; Tron, G. C. *Mol. Diversity* **2010**, *14*, 109.
- (19) Sun, H.; Liu, L.; Lu, J.; Qiu, S.; Yang, C.; Yi, H.; Wang, S. *Bioorg. Med. Chem. Lett.* **2010**, *20*, 3043.
- (20) Ajay, A.; Sharma, S.; Gupta, M. P.; Bajpai, V.; Hamidullah, ; Kumar, B.; Kaushik, M. P.; Konwar, R.; Ampapathi, R. S.; Tripathi, R. P. *Org. Lett.* **2012**, *14*, 4306.
- (21) Davis, M. R.; Singh, E. K.; Wahyudi, H.; Alexander, L. D.; Kunicki, J. B.; Nazarova, L. A.; Fairweather, K. A.; Giltrap, A. M.; Jolliffe, K. A.; McAlpine, S. R. *Tetrahedron* **2012**, *68*, 1029.
- (22) Neilsen, P. M.; Peheré, A. D.; Pishas, K. I.; Callen, D. F.; Abell, A. D. *ACS Chem. Biol.* **2013**, *8*, 353.
- (23) Tahoori, F.; Balalaie, S.; Sheikhejad, R.; Sadjadi, M.; Boloori, P. *Amino Acids* **2014**, *46*, 1033.
- (24) Goh, W. Y. L.; Chai, C. L. L.; Chen, A. *Eur. J. Org. Chem.* **2014**, 7239.
- (25) Zhang, Y.; Seigal, B. A.; Terrett, N. K.; Talbott, R. L.; Fagnoli, J.; Naglich, J. G.; Chaudhry, C.; Posy, S. L.; Vuppugalla, R.; Cornelius, G.; Lei, M.; Wang, C.; Zhang, Y.; Schmidt, R. J.; Wei, D. D.; Miller, M. M.; Allen, M. P.; Li, L.; Carter, P. H.; Vite, G. D.; Borzilleri, R. M. *ACS Med. Chem. Lett.* **2015**, *6*, 770.
- (26) Seigal, B. A.; Connors, W. H.; Fraley, A.; Borzilleri, R. M.; Carter, P. H.; Emanuel, S. L.; Fagnoli, J.; Kim, K.; Lei, M.; Naglich, J. G.; Pokross, M. E.; Posy, S. L.; Shen, H.; Surti, N.; Talbott, R.; Zhang, Y.; Terrett, N. K. *J. Med. Chem.* **2015**, *58*, 2855.
- (27) Cao, G.; Yang, K.; Li, Y.; Huang, L.; Teng, D. *Molecules* **2016**, *21*, 212.
- (28) Gabba, A.; Robakiewicz, S.; Taciak, B.; Ulewicz, K.; Broggoni, G.; Rastelli, G.; Krol, M.; Murphy, P.; Passarella, D. *Eur. J. Org. Chem.* **2017**, 60.
- (29) Raj, P. J.; Bahulayan, D. *Tetrahedron Lett.* **2017**, *58*, 2122.
- (30) Hernandez-Vazquez, E.; Chavez-Riveros, A.; Romo-Perez, A.; Ramirez-Apan, M. T.; Blanco, A. D. C.; Morales-Barcenas, R.; Duenas-Gonzalez, A.; Miranda, L. D. *ChemMedChem* **2018**, *13*, 1193.
- (31) Cruz-Lopez, O.; Temps, C.; Longo, B.; Myers, S. H.; Franco-Montalban, F.; Unciti-Broceta, A. *ACS Omega* **2019**, *4*, 21620.
- (32) Rahman, A.; Sharma, P.; Kaur, N.; Shanavas, A. K.; Neelakandan, P. P. *ChemistrySelect* **2020**, *5*, 5473.
- (33) Srinivas, A.; Rao, E. K. *Acta Chim. Slov.* **2021**, *68*, 404.
- (34) Hernandez-Vazquez, E.; Amador-Sanchez, Y. A.; Cruz-Mendoza, M. A.; Ramirez-Apan, M. T.; Miranda, L. D. *Bioorg. Med. Chem. Lett.* **2021**, *40*, 127899.
- (35) Isidro-Llobet, A.; Murillo, T.; Bello, P.; Cilibrizzi, A.; Hodgkinson, J. T.; Galloway, W. R. J. D.; Bender, A.; Welch, M.; Spring, D. R. *Proc. Natl. Acad. Sci. USA* **2011**, *108*, 6793.
- (36) Noor, A.; Huff, G. S.; Kumar, S. V.; Lewis, J. E. M.; Paterson, B. M.; Schieber, C.; Donnelly, P. S.; Brooks, H. J. L.; Gordon, K. C.; Moratti, S. C.; Crowley, J. D. *Organometallics* **2014**, *33*, 7031.
- (37) Guo, Y.; Liu, C.; Song, H.; Wang, F.; Zou, Y.; Wu, Q.; Hu, H. *RSC Adv.* **2017**, *7*, 2110.
- (38) Singh, K.; Sharma, G.; Shukla, M.; Kant, R.; Chopra, S.; Shukla, S. K.; Tripathi, R. P. *J. Org. Chem.* **2018**, *83*, 14882.
- (39) Yang, X.; Kemmink, J.; Rijkers, D. T. S.; Liskamp, R. M. J. *Bioorg. Med. Chem. Lett.* **2022**, *73*, 128887.
- (40) Selvarani, S.; Rajakumar, P.; Nagaraj, S.; Choudhury, M.; Velmurugan, D. *New J. Chem.* **2018**, *42*, 12684.
- (41) Maurya, S. K.; Rana, R. *Beilstein J. Org. Chem.* **2017**, *13*, 1106.

- (42) Weerawarna, P. M.; Kim, Y.; Kankanamalage, A. C. G.; Damalanka, V. C.; Lushington, G. H.; Alliston, K. R.; Mehzabeen, N.; Battaile, K. P.; Lovell, S.; Chang, K.; Groutas, W. C. *Eur. J. Med. Chem.* **2016**, *119*, 300.
- (43) Kankanamalage, A. C. G.; Weerawarna, P. M.; Rathnayake, A. D.; Kim, Y.; Mehzabeen, N.; Battaile, K. P.; Lovell, S.; Chang, K.; Groutas, W. C. *Proteins Struct. Funct. Bioinform.* **2019**, *87*, 579.
- (44) Campo, V. L.; Ivanova, I. M.; Carvalho, I.; Lopes, C. D.; Carneiro, Z. A.; Saalbach, G.; Schenkman, S.; da Silva, J. S.; Nepogodiev, S. A.; Field, R. A. *Tetrahedron* **2015**, *71*, 7344.
- (45) Choi, W. J.; Shi, Z.; Worthy, K. M.; Bindu, L.; Karki, R. G.; Nicklaus, M. C.; Fisher, R. J.; Burke, T. R. Jr. *Bioorg. Med. Chem. Lett.* **2006**, *16*, 5265.
- (46) Ingale, S.; Dawson, P. E. *Org. Lett.* **2011**, *13*, 2822.
- (47) Empting, M.; Avrutina, O.; Meusinger, R.; Fabritz, S.; Reinwarth, M.; Biesalski, M.; Voigt, S.; Buntkowsky, G.; Kolmar, H. *Angew. Chem. Int. Ed.* **2011**, *50*, 5207.
- (48) Pehere, A. D.; Pietsch, M.; Gütschow, M.; Neilsen, P. M.; Pedersen, D. S.; Nguyen, S.; Zvarec, O.; Sykes, M. J.; Callen, D. F.; Abell, A. D. *Chem. Eur. J.* **2013**, *19*, 7975.
- (49) Jogula, S.; Soorneedi, A. R.; Gaddam, J.; Chamakuri, S.; Deora, G. S.; Indarapu, R. K.; Ramgopal, M. K.; Dravida, S.; Arya, P. *Eur. J. Med. Chem.* **2017**, *135*, 110.
- (50) Tala, S. R.; Singh, A.; Lensing, C. J.; Schnell, S. M.; Freeman, K. T.; Rocca, J. R.; Haskell-Luevano, C. *ACS Chem. Neurosci.* **2017**, *9*, 1001.
- (51) White, A. M.; De Veer, S. J.; Wu, G.; Harvey, P. J.; Yap, K.; King, G. J.; Swedberg, J. E.; Wang, C. K.; Law, R. H. P.; Durek, T.; Craik, D. J. *Angew. Chem. Int. Ed.* **2020**, *59*, 11273.
- (52) Kulsi, G.; Sannigrahi, A.; Mishra, S.; Saha, K. D.; Datta, S.; Chattopadhyay, P.; Chattopadhyay, K. *ACS Omega* **2020**, *5*, 16395.
- (53) Cheekatla, S. R.; Thurakkal, L.; Jose, A.; Barik, D.; Porel, M. *Molecules* **2022**, *27*, 3409.
- (54) Thurakkal, L.; Mol, R.; Porel, M. *Chem. Commun.* **2023**, *59*, 7399.